

# Thiol-Methylsulfone Based Hydrogels: Enhanced Control on Gelation Kinetics for 3D Cell Encapsulation

Julieta Paez, Aleeza Farrukh, Małgorzata K. Włodarczyk-Biegun, Aránzazu del Campo

Submitted date: 22/07/2019 • Posted date: 22/07/2019

Licence: CC BY-NC-ND 4.0

Citation information: Paez, Julieta; Farrukh, Aleeza; Włodarczyk-Biegun, Małgorzata K.; del Campo, Aránzazu (2019): Thiol-Methylsulfone Based Hydrogels: Enhanced Control on Gelation Kinetics for 3D Cell Encapsulation. ChemRxiv. Preprint.

Hydrogels are useful temporal matrices for cell culture technologies. The successful mixing and encapsulation of cells within the gel requires the selection of efficient and cytocompatible gelation reactions occurring in the minute timescale under physiological conditions. The thiol-methylsulfonyl (MS) chemical reaction is introduced here as a novel chemistry to encapsulate cells in polymeric matrices. Thiol-MS crosslinking does not require a light activation step and can occur within the seconds-to-minutes timescale by adjusting the pH in the physiological range 8.0-6.6. This reaction is cytocompatible and the reaction product is hydrolytically stable in cell culture media up to 4 weeks. Cell encapsulation protocols enabling comfortable handling and yielding homogenous distribution of the embedded cells are described. All these features are relevant for the application of this crosslinking reaction to biomedical scenarios. Finally, this manuscript also compares the performance of thiol-MS hydrogels with the established thiol-maleimide and thiol-vinylsulfone hydrogels. The benefit of thiol-MS crosslinking in terms of control over hydrogelation kinetics is demonstrated.

## File list (2)

---

Manuscript\_PaezJI.pdf (692.56 KiB)

[view on ChemRxiv](#) • [download file](#)

---

SuppInformation\_PaezJI.pdf (1.84 MiB)

[view on ChemRxiv](#) • [download file](#)

---

# Thiol-Methylsulfone based Hydrogels: Enhanced Control on Gelation Kinetics for 3D Cell Encapsulation

*Julieta I. Paez,\* Aleeza Farrukh, Małgorzata K. Włodarczyk-Biegun, Aránzazu del Campo\**

Dr. Julieta I. Paez, Dr. Aleeza Farrukh, Dr. Małgorzata K. Włodarczyk-Biegun, Prof. Dr. Aránzazu del Campo.

INM – Leibniz Institute for New Materials, Campus D2-2, 66123, Saarbrücken, Germany  
E-mail: julieta.paez@leibniz-inm.de; aranzazu.delcampo@leibniz-inm.de

Prof. Dr. Aránzazu del Campo.

Saarland University, Chemistry Department, 66123 Saarbrücken, Germany

**Keywords:** 3D cell culture, thiol-mediated chemistry, coupling under physiological conditions, aromatic methylsulfones, gelation kinetics.

**Abstract:** Hydrogels are useful temporal matrices for cell culture technologies. The successful mixing and encapsulation of cells within the gel requires the selection of efficient and cytocompatible gelation reactions occurring in the minute timescale under physiological conditions. The thiol-methylsulfonyl (MS) chemical reaction is introduced here as a novel chemistry to encapsulate cells in polymeric matrices. Thiol-MS crosslinking does not require a light activation step and can occur within the seconds-to-minutes timescale by adjusting the pH in the physiological range 8.0-6.6. This reaction is cytocompatible and the reaction product is hydrolytically stable in cell culture media up to 4 weeks. Cell encapsulation protocols enabling comfortable handling and yielding homogenous distribution of the embedded cells are described. All these features are relevant for the application of this crosslinking reaction to biomedical scenarios. Finally, this manuscript also compares the performance of thiol-MS hydrogels with the established thiol-maleimide and thiol-vinylsulfone hydrogels. The benefit of thiol-MS crosslinking in terms of control over hydrogelation kinetics is demonstrated.

## 1. Introduction

Progress in 3D culture technologies and cell therapies depends on our ability to encapsulate cells in supportive microenvironments for cellular proliferation and self-organization.

Hydrogels are typically used as temporal extracellular matrix substituents in these application scenarios. A major challenge here is the development of crosslinking and biofunctionalization strategies that are efficient under physiological conditions and do not impair function of the encapsulated cells.<sup>[1]</sup> Additional requirements for practical application are simple handling, stability of precursors and crosslinked products, orthogonality to common backbone functionalities of clinically approved polymers, and tunable crosslinking kinetics to be adaptable to the particular application. A number of reactive chemistries for crosslinking under physiological conditions are nowadays available: radical-mediated acrylic polymerization,<sup>[2]</sup> amine-NHS ester coupling,<sup>[3]</sup> Schiff-base formation,<sup>[4]</sup> cycloadditions (including strain-promoted azide-cycloalkyne,<sup>[5]</sup> normal<sup>[6]</sup> and inverse<sup>[7]</sup> electron demand Diels Alder), mussel-bioinspired catechol oxidation,<sup>[8]</sup> native chemical ligation,<sup>[9]</sup> radical-mediated thiol-ene<sup>[10]</sup> and thiol-yne,<sup>[11]</sup> and nucleophilic Michael-additions.<sup>[12]</sup> However, none of these options fulfils all the previously mentioned criteria.

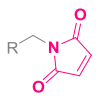
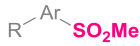
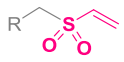
Thiol-mediated chemistry has become popular for crosslinking and preparing cell-laden hydrogels.<sup>[13]</sup> Thiols can react with activated alkenes or alkynes (thiol-ene/yne) by means of photogenerated radicals (with acrylate and norbornene groups) or through polar Michael additions (with acrylates, maleimides (Mal), and vinyl sulfones (VS)). However, photoactivated thiol-ene crosslinking has some limitations for use in combination with cells.<sup>[12c]</sup> Photodamage suffered by cells and the lack of transparency of natural tissues pose technical limitations to the application of this strategy in real scenarios. Thiol-Mal<sup>[12b]</sup> and thiol-VS<sup>[12a]</sup> coupling reactions do not require light activation.<sup>[14]</sup> However, crosslinking begins immediately upon mixing of the two components, and the reaction kinetics becomes a

critical parameter for the cell encapsulation step. The reaction should be slow enough to allow mixing and homogenization of the reactive precursors and the cells at low shear forces, and fast enough to reduce environmental stress and to avoid sedimentation of embedded cells.<sup>[15]</sup> Comfortable crosslinking times are between 30 seconds and a few minutes.<sup>[16]</sup> Thiol-Mal reaction has a very fast rate constant (see Table 1) and thiol-Mal hydrogels form within a few seconds. It has been reported that this leads to inhomogeneity of the hydrogel matrix, and lowers reproducibility in the cell response.<sup>[17]</sup> Additionally, the Mal precursor is prone to hydrolysis under mild basic conditions, and the thiol-Mal adduct (thioether succinimide linkage) undergoes retro-Michael and exchange reactions in presence of other thiols existing in culture media.<sup>[18]</sup> As consequence, gel stability cannot be maintained for long culture times. Conversely, the thiol-VS system is very stable towards hydrolysis: both VS precursor and thioether adduct are stable for long time under physiological conditions.<sup>[13c]</sup> However, thiol-VS coupling rate constant is 2-3 orders of magnitude slower than thiol-Mal. In fact, thiol-VS hydrogels form within several minutes to hours. Therefore, although the reactive VS-system can be properly mixed, cell sedimentation and clustering are commonly observed.<sup>[19]</sup> This precludes homogeneous distribution of the encapsulated cells throughout the material. Several approaches have been tested to narrow the “kinetic gap” between the thiol-Mal and thiol-VS reactions, either by changing reaction conditions (temperature, pH, buffer type and concentration, presence of catalysts or inhibitors);<sup>[17, 20]</sup> or by changing the concentration<sup>[17b, 20a]</sup> or architecture of the polymer precursor (molar mass, branching, multifunctionality).<sup>[19-20, 21]</sup> Other approaches include the tuning of the reaction rate by molecularly engineering the pKa of the thiol group<sup>[17, 20a]</sup> (changing the thiol’s molecular environment) and the use of thickeners to adjust the viscosity of gel precursors to prevent cell sedimentation.<sup>[22]</sup> Despite the progress so far, kinetic control of these systems may come at the expenses of changes in the mechanical properties of the final hydrogel, or compromised cell viability. For example, decreasing pH from 8 to 5 allowed to increase the gelation time of thiol-Mal from a few

seconds to roughly one minute; albeit with a consequent 3-fold drop of the final shear modulus  $G'$ .<sup>[17b]</sup> Moreover, 16 mM zinc chloride was added to inhibit and slow down the thiol-Mal gelation to 2-3 min; however, the needed concentration of this compound proved to be non-cytocompatible.<sup>[17b]</sup>

The thiol-methylsulfonyl (MS) reaction is an interesting alternative to thiol-Mal or thiol-VS reactions which has not been exploited for crosslinking hydrogels so far. Thiols effectively react with aromatic rings bearing MS groups under physiological conditions via a nucleophilic aromatic substitution mechanism.<sup>[23]</sup> This reaction is characterized by high yield, high chemoselectivity and the formation of a stable thio-ether product.<sup>[23a]</sup> Moreover, its reaction rate can be regulated by adjusting the pH in the range 6-9<sup>[23a]</sup> and by adjusting the electron-deficient character of the aromatic substrate bearing the MS group.<sup>[23b, 24]</sup> This reaction, originally developed for the selective blocking of thiol-containing proteins<sup>[23a]</sup> and for protein bioconjugation,<sup>[23b]</sup> has been recently applied by our group to biofunctionalize hydrogels for 2D cell culture.<sup>[25]</sup> The observed high reaction conversion and moderate reaction rate<sup>[24]</sup> of the thiol-MS chemistry as well as the good stability<sup>[23]</sup> and proven cytocompatibility<sup>[25a]</sup> of formed adducts are ideal properties for crosslinking cell-laden hydrogels. In this manuscript we study the crosslinking kinetics of thiol-MS derived poly(ethylene glycol) (PEG), and demonstrate its benefits *vs.* thiol-Mal and thiol-VS systems for cell encapsulation.

**Table 1.** Reported second-order reaction rate constants for selected nucleophilic thiol-X couplings under mild aqueous conditions.

X react. group	reaction rate $k_2$ [ $M^{-1} s^{-1}$ ]	reference
Mal 	734.0	[26]
MS 	0.4 - 16.0	[24]
VS 	0.08 - 1.0	[27]

## 2. Results and Discussion

We selected the 2-(methylsulfonyl)-5-phenyl-1,3,4-oxadiazole group as MS substrate for thiol coupling. Among reported MS heteroaromatic rings, this substrate reacts with thiols with high conversion at intermediate reaction rate (Table 1).<sup>[23b, 24]</sup> 4-arm PEG-MS macromers (20 kDa) with substitution degree >95% were synthesized at 350-mg scale in good yield after three simple synthetic steps to form two amide bonds (**Figure 1a**). The MS precursor carrying an aromatic amine was first coupled to Boc-glycine followed by Boc deprotection and coupling to PEG-NHS. Details on the synthesis, purification and characterization of intermediates and macromers are included in the Supporting Information (SI).

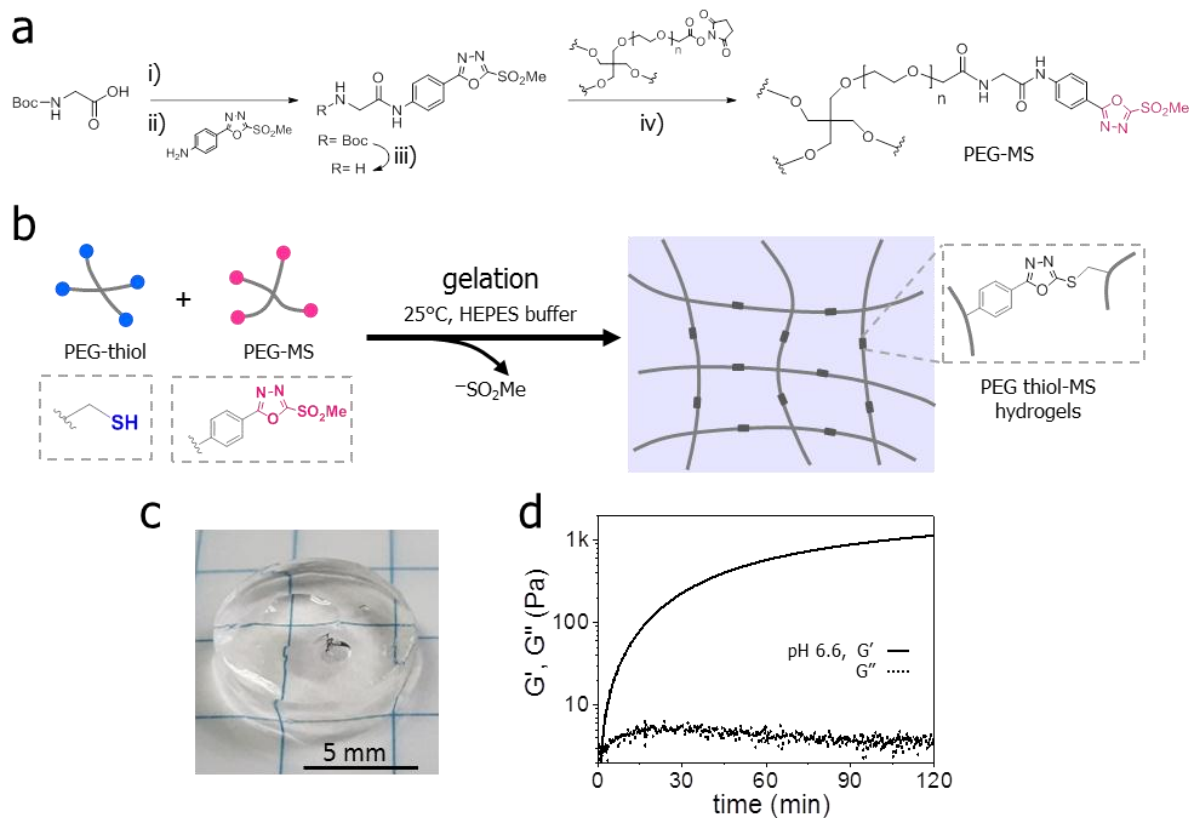


**Figure 1.** Chemical structure and properties of PEG-based thiol-MS hydrogels. **a)** Synthetic pathway to PEG-MS macromer; conditions: i) isobutyl chloroformate, NMM, THF:DMF (1:1), 0°C, 30 min; ii) r.t, overnight; iii) TFA:DCM (1:1), 0°C, 30 min; iv) DMF, NMM, r.t, N<sub>2</sub>, overnight. **b)** Schematic crosslinking of PEG-MS and PEG-thiol precursors to form PEG-thiol-MS hydrogels. **c)** Photograph of a swollen PEG-thiol-MS hydrogel. **d)** Shear storage ( $G'$ ) and loss ( $G''$ ) moduli as a function of time during gel formation. Conditions for **c-d**): 5 wt% polymer, 10 mM HEPES buffer pH 6.6,  $T = 25^\circ\text{C}$ .

The gelation of 4-arm PEG-MS and 4-arm PEG-thiol mixture was explored. Applied crosslinking conditions were 5 wt% polymer content in 10 mM HEPES buffer and pH in the 6.6 to 8.0 range, at 25°C. A 1:1 MS:thiol ratio was used for the experiments. Preliminary studies based on macroscopic observations indicated that thiol-MS gels at pH 6.6 formed a crosslinked gel within 4 min (see Figure 1d and Table 2). This is a convenient crosslinking time that enables proper mixing and homogenization of precursor solutions. At pH 6.6, the crosslinked networks reached a shear storage modulus of  $G' \sim 1$  kPa as measured by rheology (Figure 1d). Note that methanesulfinic acid is formed as byproduct of the crosslinking

reaction (demonstrated by  $^1\text{H}$  NMR and mass spectrometry analyses, see details in the Supporting Information, Figure S1 to S3). This aspect will be further addressed later in the manuscript.

**Figure 2a** compares the crosslinking kinetics of thiol-MS with that of thiol-Mal and thiol-VS systems. Experiments were performed under conditions typically used to prepare thiol-mediated gels for cell culture (5 wt% polymer, in 10 mM HEPES buffer, pH 8.0, at 25°C).<sup>[12b, 28]</sup> Under these conditions, the thiol-MS gel formed in 3-4 s (Table 2). This is a short crosslinking time, though it allowed mixing and homogenization of gel precursors. In comparison, the thiol-Mal gel required <1 s for crosslinking and inhomogeneous gels were obtained, while the thiol-VS system showed a gelation time of about 10 min and took ca 2 h to complete crosslinking. These results indicate the following trend in gelation rate: thiol-Mal > thiol-MS > thiol-VS, in agreement with reported reaction rates for model compounds,<sup>[24, 26-27]</sup> as shown in Table 1.

The values of the shear modulus of the crosslinked gels after 1 h were  $G'_{25^\circ\text{C}} = 1700$  Pa for thiol-VS, 700 Pa for thiol-MS and 480 Pa for thiol-Mal, respectively (5 wt%, pH 8.0). The higher shear modulus of thiol-MS vs. thiol-Mal hydrogels is probably due to a higher homogeneity of the former, as consequence of the slower gelation kinetics, enabling better mixing of precursors and leading to less network defects and higher crosslinking degree. This result contradicts previous reactivity studies of thiol-Mal and thiol-MS couplings on small model molecules, which were shown to have similar reaction conversions in phosphate buffer saline (PBS) pH 7.4.<sup>[23b]</sup> We hypothesized that hydrolysis of Mal groups, which occurs at basic pH, could be in part the reason for the lower mechanical properties of thiol-Mal in our studies at pH 8. To check this hypothesis, the stability of a 4 wt% PEG-Mal solution in deuterated PBS was studied by  $^1\text{H}$  NMR. Hydrolysis of Mal groups was detected from 45 min (see Figure S4 and S5 in the SI), confirming that lower shear modulus of thiol-Mal gels could



be due to Mal hydrolysis. Thiol-VS gels reached the highest shear modulus. We hypothesized that this could be related to a higher conversion or to the slower curing kinetics rendering a network with fewer defects. Similar trend in the crosslinking kinetics was observed at 37°C and pH 8.0,  $G'_{37^\circ\text{C}} = 2700$  Pa for thiol-VS, 1250 Pa for thiol-MS and 500 Pa for thiol-Mal after 1 hour reaction time (Figure S6). Altogether, these results show that thiol-MS crosslinking presents intermediate kinetics between the very fast crosslinking thiol-Mal and the slow thiol-VS derived materials. The observed crosslinking time in the range of a few seconds allows comfortable mixing and pipetting of the components at low shear forces, and this is expected to be profitable for cell encapsulation.<sup>[29]</sup>

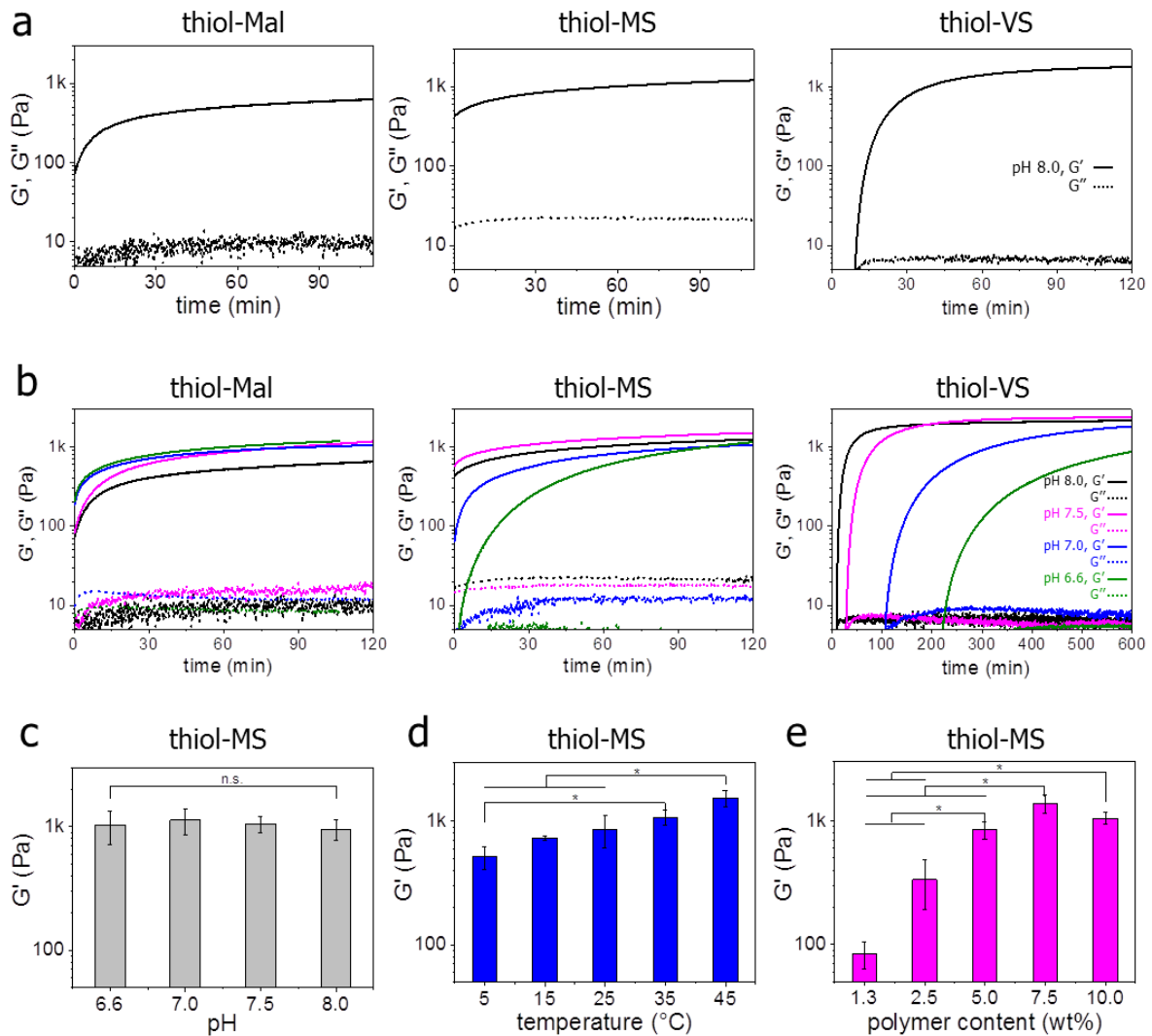


**Figure 2.** Comparison of gelation kinetics of thiol-X hydrogels under different conditions, as measured by rheology. **a)** Effect of crosslinking chemistry (at 5 wt% polymer content, pH 8.0,  $T=25^{\circ}\text{C}$ ) and **b)** effect of pH (at 5 wt% polymer content,  $T=25^{\circ}\text{C}$ ) on crosslinking kinetics and shear moduli. **c)** Final shear modulus of thiol-MS gels remains unaffected upon changing pH (conditions: 5 wt% polymer content,  $T=25^{\circ}\text{C}$ , at 2 h). **d-e)** Variation of  $G'$  of thiol-MS hydrogels with reaction parameters: **d)** temperature between 5 and 45 °C (5 wt% polymer content, pH 7.0, 1 h reaction time) and **e)** polymer content between 1.3 and 10 wt% (pH 7.5,  $T=25^{\circ}\text{C}$ , 1 h reaction time). Statistical significance analysis was performed by ANOVA followed by post-hoc Tukey test (mean  $\pm$  SD, \*  $p < 0.05$  was used for statistical significance; n.s. = not significant.)

**Table 2.** Gelation time of thiol-X hydrogels at varying pH values.

gel <sup>a)</sup>	pH			
	8.0	7.5	7.0	6.6
thiol-Mal	<1 s	1-2 s	2-3 s	5-6 s
thiol-MS	3 s	6 s	12 s	4 min
thiol-VS	8 min	22 min	88 min	190 min

<sup>a)</sup> Experiments were performed at 5 wt% polymer content, in 10 mM HEPES buffer,  $T = 25^{\circ}\text{C}$ . Gelation time was taken as the time elapsed between the mixing of the two components (30  $\mu\text{L}$  each) and the moment when pipetting of the mixture was no longer possible. Size of pipette tip = 2-200  $\mu\text{L}$ , 53 mm.

The reaction rate of the polar thiol-X coupling is dependent on pH within the pH range 6 to 9. This is due to the deprotonation of the thiol group ( $\text{pK}_a \sim 8$ ), which acts as nucleophile in these reactions.<sup>[30]</sup> This feature provides an interesting opportunity for pH-controlled curing kinetics within physiologically relevant conditions. Thiol-MS crosslinking within pH interval of 8.0-6.6 was studied. Remarkably, the pH change from 8.0 to 6.6 allowed slowing of the gelation process from a few seconds to a couple of minutes (Figure 2b, Table 2), providing an ideal experimental time window for 3D cell encapsulation applications. In contrast, thiol-Mal gelation time only varied within a few seconds, while thiol-VS ranged from a few minutes to a couple of hours in the same pH range (Figure 2b, Table 2). These results highlight the advantages of thiol-MS gels in terms of handling and adaptability to application specifications *versus* the thiol-Mal and thiol-VS as established, state-of-the-art formulations.

The final shear modulus of thiol-MS crosslinked hydrogels remained unaffected by the working pH in the interval  $\text{pH} = 8.0\text{-}6.6$  (Figure 2c and S7,  $G'$  after 2 h of gelation ca 1 kPa). This proves that the handling of thiol-MS gels can be tuned with pH without changing materials properties and without compromising the final stability of the gel. In comparison, thiol-Mal system showed a drop in  $G'$  at pH 8.0 but similar final shear modulus at  $\text{pH} = 7.5\text{-}6.6$  (Figure S8), while thiol-VS showed a clear trend of slower gelation kinetics and decreased shear modulus with decreasing pH (Figure S9).

The dependence of gelation kinetics and shear modulus of thiol-MS gels with gelation temperature and polymer concentration was also studied. A temperature decrease from 45°C to 5°C allowed a decrease in shear modulus from 1540 to 520 Pa (Figure 2d and S10, measured at pH 7.0, 1 h reaction time) and an increase in the gelation time from 7 to 30 s (Table S1). Increasing polymer content from 1.3 to 10 wt% led to shortening of the gelation time from 18 to 2 s (Figure 2e and Table 2, measured at pH 7.5 and 25°C). The increase of the polymer content raises the probability of reaction partners to form the new crosslinks and increases the reaction rate.  $G'$  also increased from 85 to 1400 Pa with an increase in the polymer concentration from 1.3 to 7.5 wt% and, surprisingly, slightly dropped for polymer concentration of 10 wt%. This result was surprising, since mixing of the 10 wt% precursor mixture appeared to be uncomplicated and no inhomogeneity issues were expected. To get a deeper insight, we measured the pH of the resulting gels (see Figure S11a). We found that the pH of the thiol-MS gels after polymerization decreased with increasing polymer concentration. Gels between 1.3-7.5 wt% showed a pH between 7.5-6.5, while gels at 10 wt% had a pH around 5.1. Note that the pH of the mixture was buffered at 10 mM HEPES in all cases. The drop in pH during gelation can be explained by the release of methanesulfinic acid as leaving group during thiol-MS coupling (Figure S1 to S3). At high polymer content (10 %), the leaving group is produced at higher concentration, leading to an acidic pH of the crosslinking reaction and, consequently, to lower crosslinking degree and final shear modulus value. This effect could be avoided by increasing the buffer capacity of the crosslinking medium. Using 50 mM HEPES buffer concentration and increasing polymer content from 1.3-10 wt% resulted in increased  $G'$  from 100 to 1300 Pa while the pH of the gels varied from 7.3 to 6.8 (Figure S11b). Note that these conditions are also cytocompatible (see Figure S13 and Ref [31]).

**Table 3.** Swelling ratio in water of thiol-X hydrogels.

gel <sup>a)</sup>	swelling ratio (SR)	
	[mg water per mg gel]	relative value
thiol-Mal	77.1 ± 3.0	1.7
thiol-MS	46.0 ± 2.8	1.0
thiol-VS	49.3 ± 1.4	1.1

<sup>a)</sup> Conditions: 5 wt% polymer content;  $n=3$ .

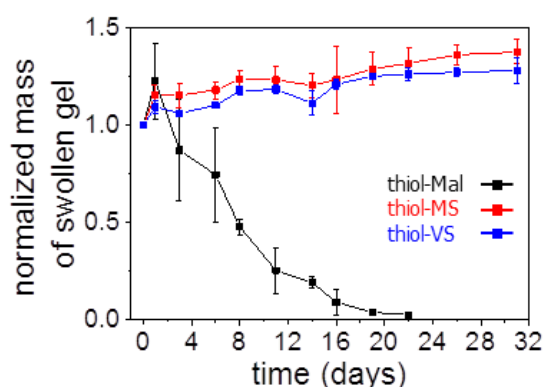


**Figure 3.** Hydrolytic stability of thiol-X gels. Gels (prepared at 5 wt% polymer content,  $n=3$ ) were incubated in cell culture medium at 37°C for >4 weeks and the mass of the swollen gel was measured.

The swelling ratio (SR) of 5 wt% thiol-MS gels was measured in water. A swelling of  $46.0 \pm 2.8$  mg water per mg polymer was obtained (Table 3). Thiol-VS gels displayed similar SR values, while thiol-Mal swelled ca 1.7-fold more. The higher swelling of thiol-Mal gels agrees with their lower crosslinking degree revealed by the rheology measurements. The similar swelling values of thiol-MS and thiol-VS gels, inspite of lower crosslinking degree of thiol-MS gels, can be explained by the hydrophobic character of the aromatic thioether crosslinks in thiol-MS gels.

The hydrolytic stability is a relevant material property for hydrogels designed for 3D cell culture. Stability experiments with 5 wt% thiol-X gels were performed by gravimetric

analysis of gels after incubation in cell culture medium (RPMI, containing FBS) at 37°C for >4 weeks (**Figure 3**). The mass of swollen thiol-MS gels reached 1.2 times the initial mass during the first 2 weeks and 1.4 times at the week 4, indicating little gel erosion and high hydrolytic stability of the thiol-MS gel system. Note that the long-term stability of the gels is advantageous for long term cell culture, and allows specific tuning of degradation kinetics by copolymerization with degradable peptides.<sup>[12b]</sup> The stability of thiol-MS system was similar to that of thiol-VS, which is typically used for long term cultures,<sup>[12a]</sup> and much higher than the stability of thiol-Mal gels (1.2-fold swelling in 2 days followed by hydrogel disintegration at day 18).<sup>[32]</sup> The hydrolysis of thiol-Mal gels is related to the low stability of the thioether succinimide bond, which undergoes retro-Michael and exchange reactions in presence of other soluble thiols existing in cell culture media.<sup>[18]</sup> Our results are in agreement with reported studies on model MS compounds, showing superior stability of thio-heteroaromatic conjugates resulting from thiol-MS coupling *versus* thiol-Mal ones under physiological conditions.<sup>[23b]</sup> Thiol-MS gels with 10 wt% polymer content remained hydrolytically stable over >6 weeks (results not shown).

Thiol-MS hydrogels were tested as matrices for cell encapsulation. We followed reported protocols used for 3D cell encapsulation with thiol-Mal gels.<sup>[12b, 28]</sup> The PEG-MS precursor was first incubated with the cell adhesive cyclo(RGDfC) peptide, then mixed with L929 fibroblasts, and finally mixed with an enzymatically cleavable dithiol peptide (VPM) as crosslinker. A composition of 4 wt% PEG-MS, 1 mM RGD peptide and 3.14 mM VPM was used.<sup>[12b, 28]</sup> Upon mixing, the solution remained low viscous for a few seconds, enabling homogenization by pipetting at low shear forces. A stable gel formed within 15 min, as visualized by naked eye. The distribution of the cells within the hydrogel was analyzed by Z-stack imaging at a confocal microscope. A uniform distribution of cells across the thickness of the hydrogel was observed (**Figure 4a**). Live/dead assays performed on cells encapsulated for

1 day into thiol-MS gels proved the cytocompatibility of our material (>90% viability, Figure 4b and c). These results indicate that the crosslinking kinetics of PEG-MS system is very convenient for obtaining homogeneous constructs at physiological and cytocompatible experimental conditions. Achieving a homogeneous cell density within an artificial matrix is relevant for modulating the behavior of delivered cells, for example, in injectable systems.<sup>[15]</sup> Similar experiments performed with thiol-Mal hydrogels resulted in immediate curing upon mixing of the precursors, impeding homogenization and leading to cell agglomeration at the upper part of the gel (Figure 4a). On the other hand, the thiol-VS system allowed for adequate mixing, but the slow gelation kinetics lead to cell sedimentation at the bottom of the gel during the curing time (Figure 4a). These results are in line with previous reports by Peyton et al<sup>[17a]</sup> on the effect of crosslinking rate on the distribution of fluorescent beads encapsulated into thiol-Mal hydrogels, and by Shikanov et al<sup>[19]</sup>, who indicated the need of flipping around thiol-VS gels during curing to avoid cell settling. In this context, thiol-MS hydrogels show ideal kinetics and overcome these inconveniences. Cells embedded in thiol-MS hydrogels after 3 days of culture remained homogeneously distributed and showed less clustering than in the other two systems (see Figure S12).

In order to prove that cells cultured in thiol-MS hydrogels remained functional, a migration assay was performed. L929 fibroblast spheroids were encapsulated in the degradable thiol-MS hydrogels,<sup>[28]</sup> cultured for 3 days, fixed and stained.<sup>[28]</sup> Cell migration distance from the spheroid was quantified as an indication for invasiveness through 3D hydrogels. Cell motility in 3D matrices is reported to decrease with a decrease in pore size of the gel or with an increase in network crosslinking and matrix hydrolytic stability.<sup>[33]</sup> Cells in the encapsulated spheroid remained viable, recognized the RGD ligand bound to the matrix, enzymatically hydrolyzed the gel network and actively migrated through 3D thiol-MS hydrogels. They covered a distance of  $d \sim 425 \pm 38 \mu\text{m}$  after 3 days of culture (Figure 4d and f). We compared these

results with those obtained for thiol-Mal and thiol-VS as materials for 3D cell encapsulation. The migration distance was  $\sim 470 \pm 55 \mu\text{m}$  for thiol-Mal and  $\sim 360 \pm 48 \mu\text{m}$  for thiol-VS systems, respectively (Figure 4f). This result can be attributed to the differences in the gel shear storage modulus (note that  $G'_{37^\circ\text{C}} = \text{VS} > \text{MS} > \text{Mal}$ , as shown in Figure S6) and in the hydrolytic stability ( $\text{MS}=\text{VS} \gg \text{Mal}$ , Figure 3). A lower crosslinking density and a faster degradation turn the matrix more invasive by cells,<sup>[34]</sup> and lead to longer migrated distances. Altogether, our results demonstrate the potential of novel thiol-MS hydrogels as valuable alternative biomaterial for 3D cell encapsulation.



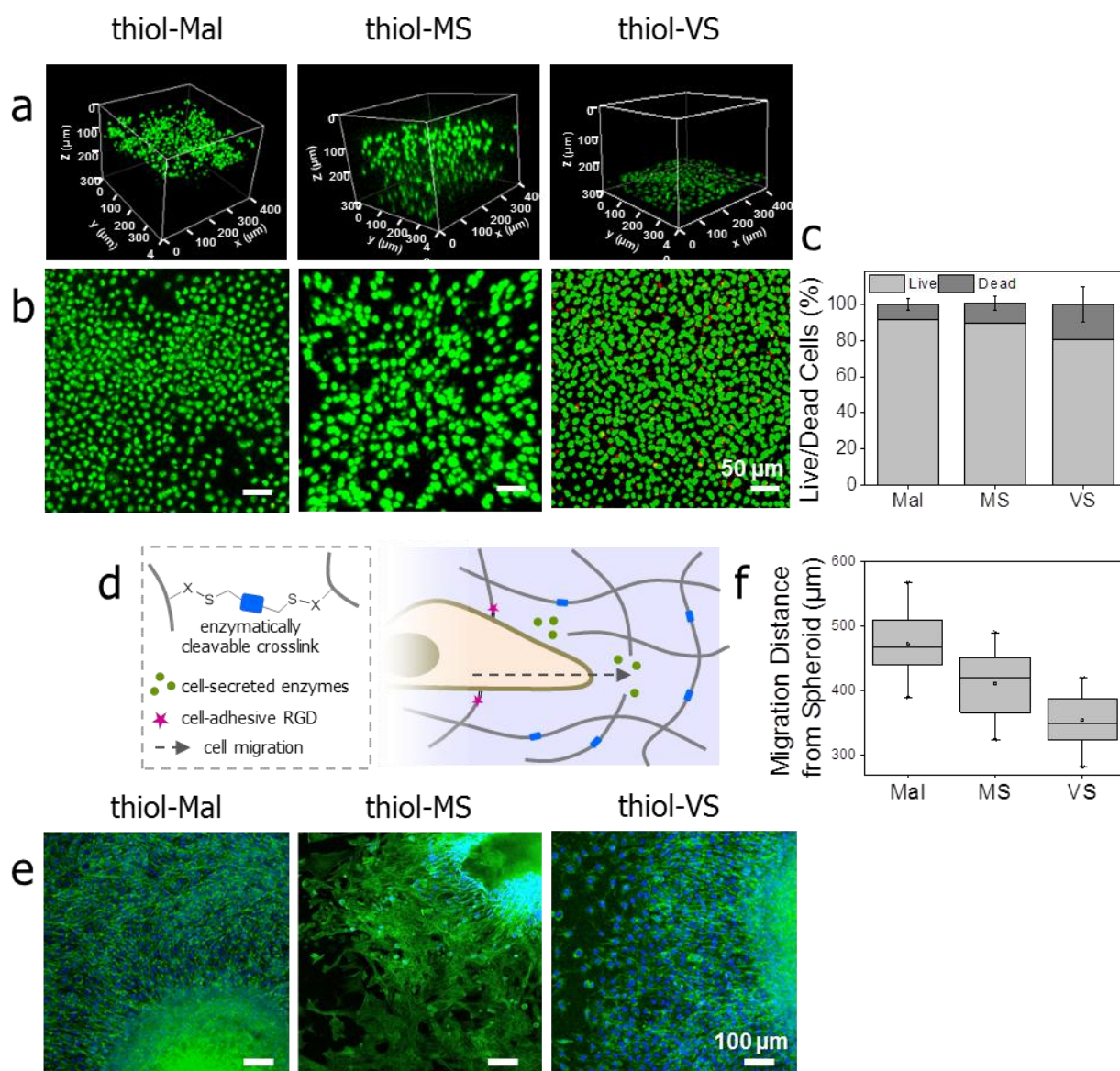


**Figure 4.** L929 fibroblast encapsulated in enzymatically cleavable thiol-X PEG hydrogels. **a,b**) Z-stack fluorescence images of a live (green)/dead (red) assay of fibroblasts encapsulated for 1 day in the hydrogels. **c**) Quantification of cell viability. **d**) Schematics of enzymatically cleavable gels used for encapsulation of cell spheroids. **e**) Fluorescence images of cells migrating out of encapsulated spheroids after 3 days of culture. Green: FITC-phalloidin (actin fibers), blue: DAPI (nucleus). **f**) Quantification of migration distance from **e**).

### 3. Conclusions

The thiol-MS reaction is suitable for crosslinking hydrogels and for cell-encapsulation. This reaction presents intermediate kinetics between thiol-Mal and thiol-VS systems and proceeds at high conversion. The resulting reaction product has good hydrolytic stability and cytocompatibility. Under aqueous mild conditions, the thiol-MS reaction is orthogonal to

alcohols, amines, carboxylic acids and acrylate functional groups,<sup>[23a, 25a, 25b]</sup> which allows the application of this crosslinking mechanism to almost any natural polymeric backbone of interest in the biomedical field. The reactivity of thiol-MS pair can be regulated by the working pH and by selecting different MS aromatic substrates.<sup>[23b]</sup> All these properties together make thiol-MS a superior alternative to thiol-MA and thiol-VS for 3D cell encapsulation. Beyond 3D culture applications, thiol-MS chemistry can be envisioned as an efficient way of generating supporting matrices for implantable or injectable cell therapy constructs of clinical interest.

### **Acknowledgements**

The authors thank Dr. Josef Zapp (Saarland University) and Dr. Judith Hoffmann (HIPS) for their help with 500-MHz NMR measurements; Ms. Rebecca Ludwig for technical assistance in organic synthesis of precursors, MSc. Maria Villiou for Figure S13, Dr. Claudia Fink-Straube and Mrs. Ha Rimbach-Nguyen (Chemical Analytics) for mass spectrometry measurements; as well as Dr. Roshna Vakeel and Dr. Samuel Pearson (INM) for constructive discussions. We are grateful to the European Union's Horizon 2020 research and innovation programme under the FET PROACTIVE grant agreement no. 731957 (Mechano-Control) and to DFG (Project no. 422041745) for their financial support.

### **Conflict of interest**

There are no conflicts of interest to declare.

## References

- [1] a) C. M. Madl, S. C. Heilshorn, *Adv. Funct. Mater.* **2018**, 28, 1706046; b) S. A. Fisher, A. E. G. Baker, M. S. Shoichet, *J. Am. Chem. Soc.* **2017**, 139, 7416.
- [2] C. A. Durst, M. P. Cuchiara, E. G. Mansfield, J. L. West, K. J. Grande-Allen, *Acta Biomater.* **2011**, 7, 2467.
- [3] K. W. M. Boere, M. M. Blokzijl, J. Visser, J. E. A. Linssen, J. Malda, W. E. Hennink, T. Vermonden, *J. Mater. Chem. B* **2015**, 3, 9067.
- [4] a) Y.-H. Ma, J. Yang, B. Li, Y.-W. Jiang, X. Lu, Z. Chen, *Polym. Chem.* **2016**, 7, 2037; b) D. D. McKinnon, D. W. Domaille, J. N. Cha, K. S. Anseth, *Adv. Mater.* **2014**, 26, 865; c) G. N. Grover, J. Lam, T. H. Nguyen, T. Segura, H. D. Maynard, *Biomacromolecules* **2012**, 13, 3013.
- [5] C. A. DeForest, B. D. Polizzotti, K. S. Anseth, *Nat. Mater.* **2009**, 8, 659.
- [6] L. J. Smith, S. M. Taimoory, R. Y. Tam, A. E. G. Baker, N. Bintah Mohammad, J. F. Trant, M. S. Shoichet, *Biomacromolecules* **2018**, 19, 926.
- [7] D. L. Alge, M. A. Azagarsamy, D. F. Donohue, K. S. Anseth, *Biomacromolecules* **2013**, 14, 949.
- [8] J. H. Cho, J. S. Lee, J. Shin, E. J. Jeon, S. An, Y. S. Choi, S.-W. Cho, *Adv. Funct. Mater.* **2018**, 28, 1705244.
- [9] J. P. Jung, A. J. Sprangers, J. R. Byce, J. Su, J. M. Squirrell, P. B. Messersmith, K. W. Eliceiri, B. M. Ogle, *Biomacromolecules* **2013**, 14, 3102.
- [10] X.-H. Qin, X. Wang, M. Rottmar, B. J. Nelson, K. Maniura-Weber, *Adv. Mater.* **2018**, 30, 1705564.
- [11] A. Skardal, M. Devarasetty, H.-W. Kang, I. Mead, C. Bishop, T. Shupe, S. J. Lee, J. Jackson, J. Yoo, S. Soker, A. Atala, *Acta Biomater.* **2015**, 25, 24.
- [12] a) M. P. Lutolf, G. P. Raeber, A. H. Zisch, N. Tirelli, J. A. Hubbell, *Adv. Mater.* **2003**, 15, 888; b) E. A. Phelps, N. O. Enemchukwu, V. F. Fiore, J. C. Sy, N. Murthy, T. A.

- Sulchek, T. H. Barker, A. J. García, *Adv. Mater.* **2012**, 24, 64; c) L. J. Macdougall, M. M. Pérez-Madrigal, M. C. Arno, A. P. Dove, *Biomacromolecules* **2018**, 19, 1378; d) P. M. Kharkar, K. L. Kiick, A. M. Kloxin, *Polym. Chem.* **2015**, 6, 5565.
- [13] a) D. L. Alge, K. S. Anseth, in *Thiol-X Chemistries in Polymer and Materials Science*, The Royal Society of Chemistry **2013**, p. 165; b) D. P. Nair, M. Podgórski, S. Chatani, T. Gong, W. Xi, C. R. Fenoli, C. N. Bowman, *Chem. Mater.* **2014**, 26, 724; c) P. M. Kharkar, M. S. Rehmann, K. M. Skeens, E. Maverakis, A. M. Kloxin, *ACS Biomater. Sci. Eng.* **2016**, 2, 165.
- [14] J. Su, *Gels* **2018**, 4, 72.
- [15] L. Haines-Butterick, K. Rajagopal, M. Branco, D. Salick, R. Rughani, M. Pilarz, M. S. Lamm, D. J. Pochan, J. P. Schneider, *Proc. Natl. Acad. Sci. U.S.A.* **2007**, 104, 7791.
- [16] a) M. Patenaude, S. Campbell, D. Kinio, T. Hoare, *Biomacromolecules* **2014**, 15, 781; b) M. Patenaude, N. M. B. Smeets, T. Hoare, *Macromol. Rapid Commun.* **2014**, 35, 598.
- [17] a) L. E. Jansen, L. J. Negrón-Piñeiro, S. Galarza, S. R. Peyton, *Acta Biomater.* **2018**, 70, 120; b) N. J. Darling, Y. S. Hung, S. Sharma, T. Segura, *Biomaterials* **2016**, 101, 199.
- [18] a) S. C. Alley, D. R. Benjamin, S. C. Jeffrey, N. M. Okeley, D. L. Meyer, R. J. Sanderson, P. D. Senter, *Bioconjugate Chem.* **2008**, 19, 759; b) A. D. Baldwin, K. L. Kiick, *Bioconjugate Chem.* **2011**, 22, 1946.
- [19] J. Kim, Y. P. Kong, S. M. Niedzielski, R. K. Singh, A. J. Putnam, A. Shikanov, *Soft Matter* **2016**, 12, 2076.
- [20] a) M. P. Lutolf, J. A. Hubbell, *Biomacromolecules* **2003**, 4, 713; b) P. M. Kharkar, A. M. Kloxin, K. L. Kiick, *J. Mater. Chem. B* **2014**, 2, 5511.
- [21] S. A. Stewart, M. B. Coulson, C. Zhou, N. A. D. Burke, H. D. H. Stöver, *Soft Matter* **2018**, 14, 8317.

- [22] D. M. Headen, J. R. García, A. J. García, *Microsyst. Nanoeng.* **2018**, 4, 17076.
- [23] a) D. Zhang, N. O. Devarie-Baez, Q. Li, J. R. Lancaster, M. Xian, *Org. Lett.* **2012**, 14, 3396; b) N. Toda, S. Asano, C. F. Barbas, *Angew. Chem., Int. Ed.* **2013**, 52, 12592.
- [24] X. Chen, H. Wu, C.-M. Park, T. H. Poole, G. Keceli, N. O. Devarie-Baez, A. W. Tsang, W. T. Lowther, L. B. Poole, S. B. King, M. Xian, C. M. Furdui, *ACS Chem. Biol.* **2017**, 12, 2201.
- [25] a) A. Farrukh, J. I. Paez, M. Salierno, A. del Campo, *Angew. Chem. Int. Ed.* **2016**, 55, 2092; b) A. Farrukh, J. I. Paez, M. Salierno, W. Fan, B. Berninger, A. del Campo, *Biomacromolecules* **2017**, 18, 906; c) J. I. Paez, A. Farrukh, O. Ustahüseyin, A. del Campo, in *Biomaterials for Tissue Engineering: Methods and Protocols* (Ed: K. Chawla), Springer New York, New York, NY **2018**, p. 101.
- [26] F. Saito, H. Noda, J. W. Bode, *ACS Chem. Biol.* **2015**, 10, 1026.
- [27] H. Wang, F. Cheng, M. Li, W. Peng, J. Qu, *Langmuir* **2015**, 31, 3413.
- [28] A. Farrukh, J. I. Paez, A. del Campo, *Adv. Funct. Mater.* **2019**, 29, 1807734.
- [29] H. J. Kong, M. K. Smith, D. J. Mooney, *Biomaterials* **2003**, 24, 4023.
- [30] M. H. Stenzel, *ACS Macro Lett.* **2013**, 2, 14.
- [31] S. H. Chen, A. Chao, C. L. Tsai, S. C. Sue, C. Y. Lin, Y. Z. Lee, Y. L. Hung, A. S. Chao, A. J. Cheng, H. S. Wang, T. H. Wang, *Mol. Ther. - Methods Clin. Dev.* **2019**, 13, 99.
- [32] N. Boehnke, C. Cam, E. Bat, T. Segura, H. D. Maynard, *Biomacromolecules* **2015**, 16, 2101.
- [33] P.-H. Wu, D. M. Gilkes, D. Wirtz, *Annu. Rev. Biophys.* **2018**, 47, 549.
- [34] M. P. Lutolf, J. L. Lauer-Fields, H. G. Schmoekel, A. T. Metters, F. E. Weber, G. B. Fields, J. A. Hubbell, *Proc. Natl. Acad. Sci. U.S.A.* **2003**, 100, 5413.

Manuscript\_PaezJI.pdf (692.56 KiB)

[view on ChemRxiv](#) • [download file](#)

---

Supporting Information for the article:

**Thiol-Methylsulfone based Hydrogels: Enhanced Control on Gelation Kinetics for 3D Cell Encapsulation**

*Julieta I. Paez\**, *Aleeza Farrukh*, *Małgorzata K. Włodarczyk-Biegun* and *Aránzazu del Campo\**

## 1. Chemical Synthesis

### 1.1. Materials and methods

Chemicals and solvents were purchased from Fluka Chemie AG (D-82024 Taufkirchen), Merck KGaA (D-64271 Darmstadt), ABCR (D-76189 Karlsruhe), Acros Organics (B-2440 Geel) and Sigma-Aldrich Chemie GmbH (D-89555 Steinheim). Solvents had p.a. purity and were used as purchased unless specified. 4-(5-(methylsulfonyl)-1,3,4-oxadiazol-2-yl)aniline was purchased from Ark Pharm USA. 4-arm (20kDa), polyethyleneglycol (PEG) polymers functionalized with maleimide (PEG-Mal), vinylsulfone (PEG-VS), thiol (PEG-SH) and succinimidyl carboxymethyl ester (PEG-NHS); and linear (5kDa) methoxylated PEG polymer analogues functionalized with NHS, Mal and SH groups were purchased from Jenkem USA. Buffer solutions were freshly prepared. 10 mM HEPES buffers (pH 8.0; 7.5, 7.0 and 6.6) were used, unless otherwise stated.

Deuterated solvents were obtained from Deutero GmbH Germany (D-56288 Kastellaun). Deuterated phosphate-buffer saline (d-PBS) was prepared by dissolving the proper amount of disodium phosphate, monosodium phosphate, sodium chloride and potassium chloride in D<sub>2</sub>O; followed by pD adjustment using 20 % DCl solution (Merck) until reaching pD values of 8.0; 7.4; 7.0; and 6.0. pH value was monitored by pH-meter and the following correction factor was applied:  $pD = pH_{obs} + 0.4$ .<sup>[1]</sup>

Thin layer chromatography (TLC) plates (ALUGRAM® SIL G/UV254) and silica gel for column chromatography (60Å pore size, 63-200µm particle size) was obtained from Macherey-Nagel, (D-52355 Düren) Germany. TLC plates were observed under 254 or 365 nm light. HPLC analysis and purification of the compounds were performed with a HPLC JASCO 4000 (Japan) equipped with a diode array, UV-Vis detector and fraction collector. Reprosil C18 columns were used for semi-preparative (250 × 25 mm) and analytical (250 × 5 mm) runs. Solvent gradients using combination of the following eluents were used: solvent A (MilliQ water + 0.1% TFA) and solvent B (95% ACN/5% MilliQ water + 0.1% TFA), typically over 40 min duration. Purification of modified polymers was typically performed by dialysis against acetone and water. Spectra/Por 3 dialysis tubing (molecular weight cut-off MWCO= 3.5 kDa) from Spectrum Inc. was used.

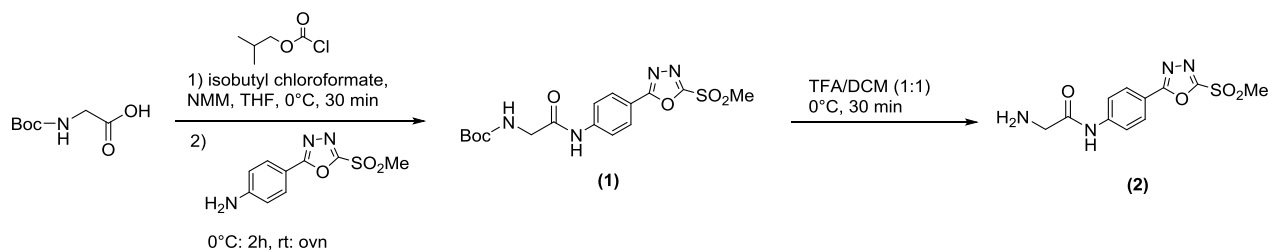
Solution <sup>1</sup>H-NMR and <sup>13</sup>C-NMR spectra were recorded at 25 °C on a Bruker Avance 300 MHz or on a Bruker Avance III UltraShield 500 MHz. The latter was equipped with a He-cooled 5 mm TCI-CryoProbe, a proton-optimized triple resonance NMR ‘inverse’ probe with external water cooling unit (CP TCI 500S2, H-C/N-D-05 Z). Unless otherwise stated, all



measurements were taken at 298K, tetramethylsilane (TMS) ( $\delta = 0$  ppm) was employed as internal reference. The chemical shifts are given in parts per million and the coupling constants in Hertz. The following abbreviations are used: *s*-singlet, *d*-doublet, *t*-triplet, *q*-quartet, *m*-multiplet. The degree of substitution of PEG polymer was calculated by end-group determination. The integral of the signal corresponding to the PEG backbone (3.70-3.40 ppm) was set to 440H and compared with the integral of the protons corresponding to the incorporated molecule **2** (the aromatic -CHs at 8.10-7.70 ppm and the methylene at 4.20 ppm). Functionalization degrees of >90% and yields of >95% were obtained in all cases. Data was analyzed in MestReNova.

Mass spectra were recorded with Agilent Technologies 1260 Infinity Liquid Chromatography/Mass Selective Detector (LC/MSD) and 6545 Accurate-Mass Quadrupole Time-of-Flight (LC/Q-TOF-MS) using electrospray chemical ionization.

## 1.2. Chemical Synthesis Protocols



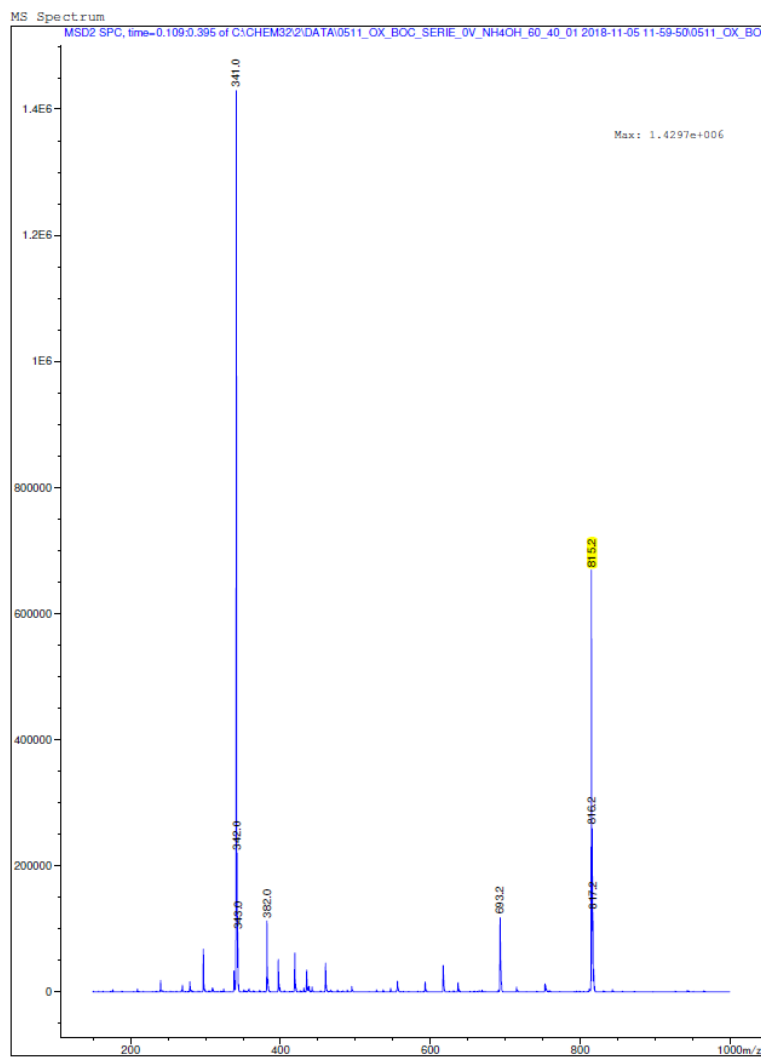
### 1.2.1. Synthesis of *tert*-butyl (2-((4-(5-(methylsulfonyl)-1,3,4-oxadiazol-2-yl)phenyl)amino)-2-oxoethyl) carbamate (**1**):

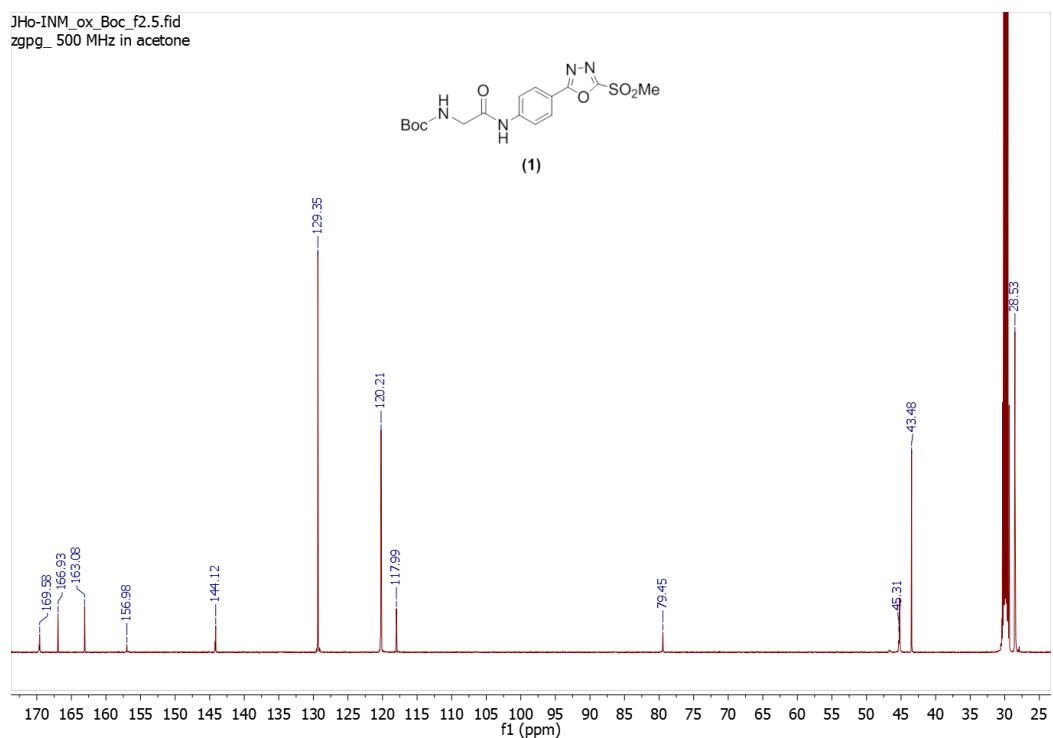
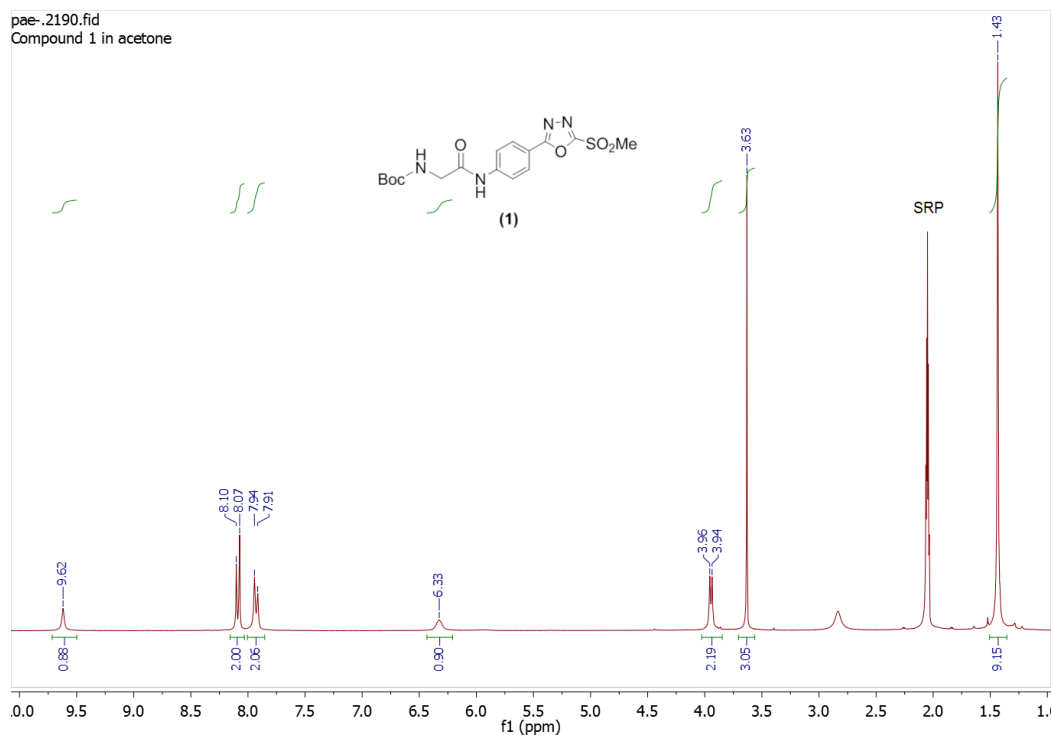
The following protocols were applied with some modifications: see ref.<sup>[2]</sup> Boc-Gly-OH (1 eq., 2.28 mmol, 0.394 g) was dissolved in 6 mL (1:1) mixture of anhydrous THF /dry DMF at 0 °C, and isobutyl chloroformate (1.2 eq, 2.85 mmol, 0.314 mL) and *N*-methylmorpholine (2.6 eq, 5.7 mmol, 0.627 mL) were carefully added to the solution with syringe under nitrogen atmosphere and the suspension was stirred for 30 minutes. A solution of 4-(5-(methylsulfonyl)-1,3,4-oxadiazol-2-yl)aniline (0.25 eq, 0.57 mmol, 0.136 g) in (1:1) THF/DMF (3 mL) was added dropwise to the mixture and stirred for additional 2h at 0 °C, then overnight at room temperature. Saturated NaHCO<sub>3</sub> was added and the reaction mixture was extracted with ethyl acetate (2 x 30 mL). The combined organic phase was washed with water (3 x 30 mL) and brine; dried over sodium sulfate, filtered, evaporated, and purified by preparative HPLC (5B to 95B 280 nm, rt= 28 min) to obtain a white solid after freeze-drying, 165 mg (yield= 73%).

ESI-MS<sup>+</sup>: 815.2 (2M+Na).

$^1\text{H-NMR}$  (300 MHz, acetone- $d_6$ ,  $\delta$  [ppm]) = 9.62 (1H, s, -NH amide); 8.10 (2H, pseudo-d, -CH Ar); 7.92 (2H, pseudo-d, -CH Ar); 6.32 (1H, pseudo-t, -NH amide); 3.93 (2H, pseudo-d, -CH<sub>2</sub>); 3.63 (3H, s, -SO<sub>2</sub>Me); 1.43 (9H, s, -tBu).

$^{13}\text{C-NMR}$  (125 MHz, acetone- $d_6$ ,  $\delta$  [ppm]) = 169.58; 166.93; 163.08; 156.98; 144.12; 129.35; 120.21; 117.99; 79.45; 45.31; 43.48; 28.53.





### 1.2.2. Synthesis of 2-amino-N-(4-(5-(methylsulfonyl)-1,3,4-oxadiazol-2-yl)phenyl)acetamide (2):

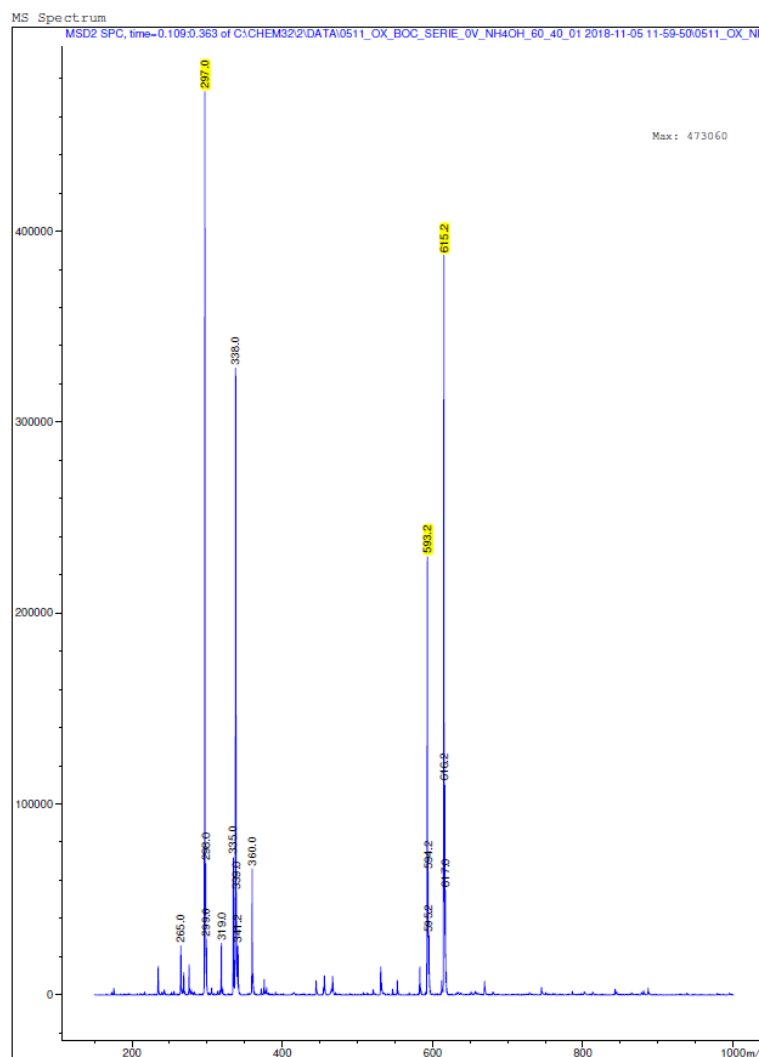
Compound **1** (165 mg) was dissolved in 1:1 TFA/DCM (2mL) and stirred at room temperature. Completion of reaction was followed by TLC (30 min). The crude was evaporated under nitrogen flow and the final product was obtained after HPLC purification (5B to 95B 280 nm, rt= 18 min). A white solid was obtained, 122 mg, yield= 99%. The pure

compound was immediately coupled to the PEG-NHS polymer; otherwise decomposition was observed.

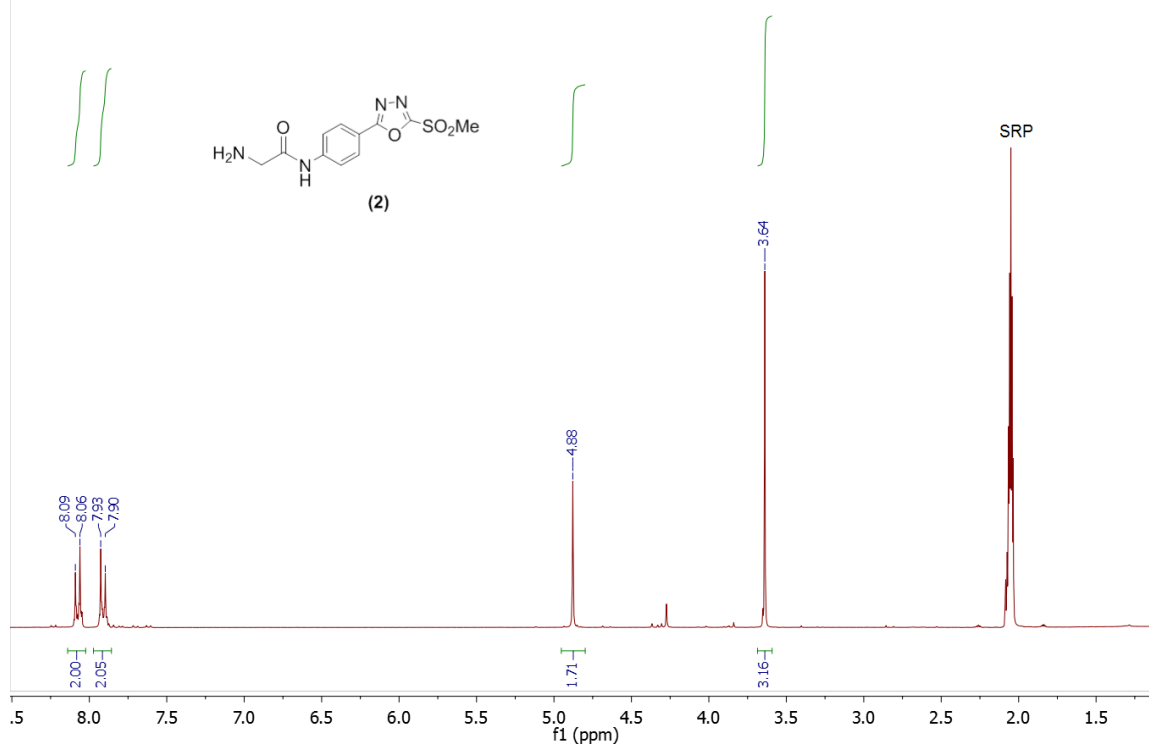
ESI-MS+: 297.1 (M+H), 593.2 (2M+H), 615.2 (2M+Na).

$^1\text{H-NMR}$  (300 MHz, acetone- $d_6$ ,  $\delta$  [ppm]) = 8.07 (2H, pseudo-d, -CH Ar); 7.92 (2H, pseudo-d, -CH Ar); 4.32 (2H, s, -CH<sub>2</sub>); 3.64 (3H, s, -SO<sub>2</sub>Me).

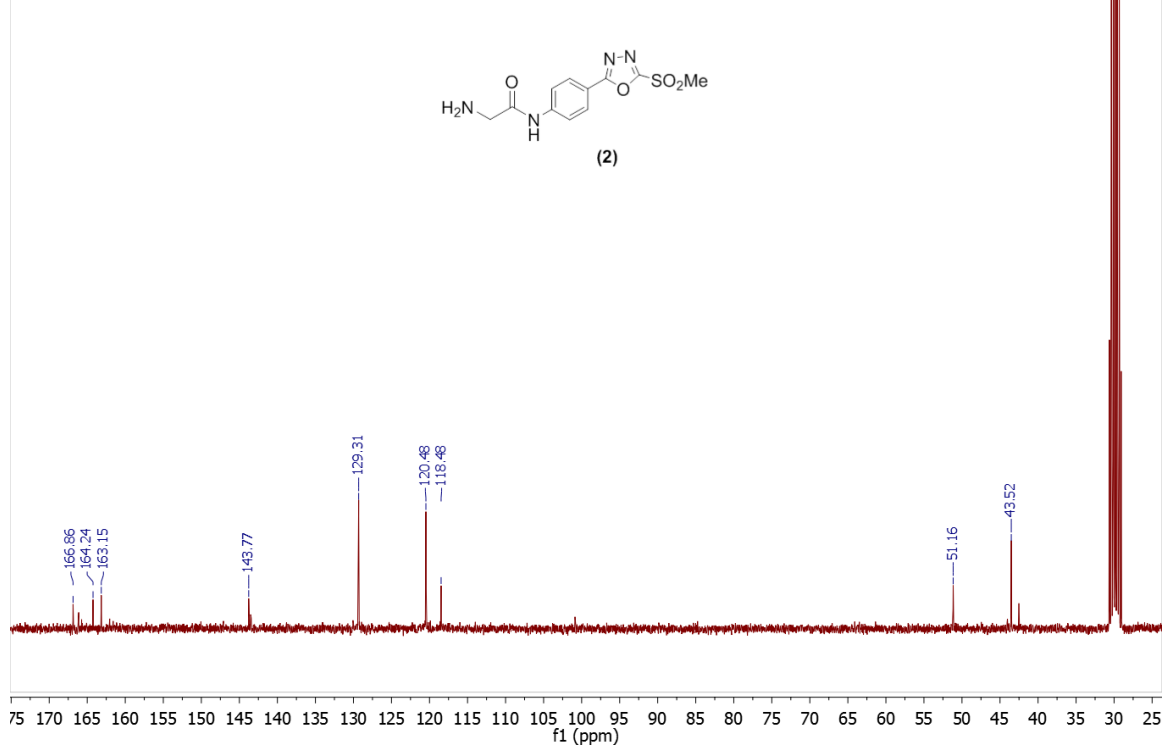
$^{13}\text{C-NMR}$  (75 MHz, acetone- $d_6$ ,  $\delta$  [ppm]) = 166.86; 164.24; 163.15; 143.77; 129.31; 120.48; 118.48; 51.16; 43.52.



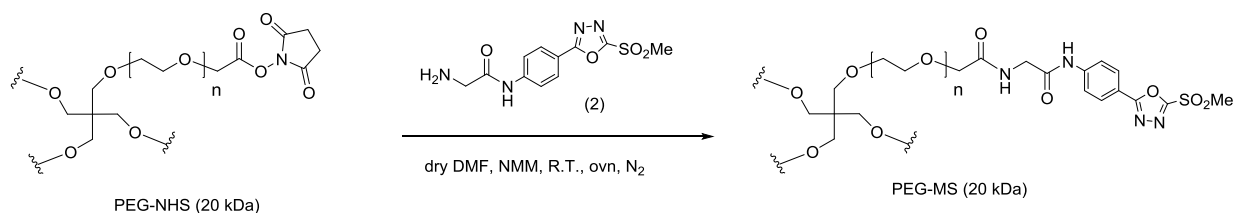
pae-.3220.fid  
Compound 2 in acetone



pae-.3141.fid  
Compound 2 in acetone

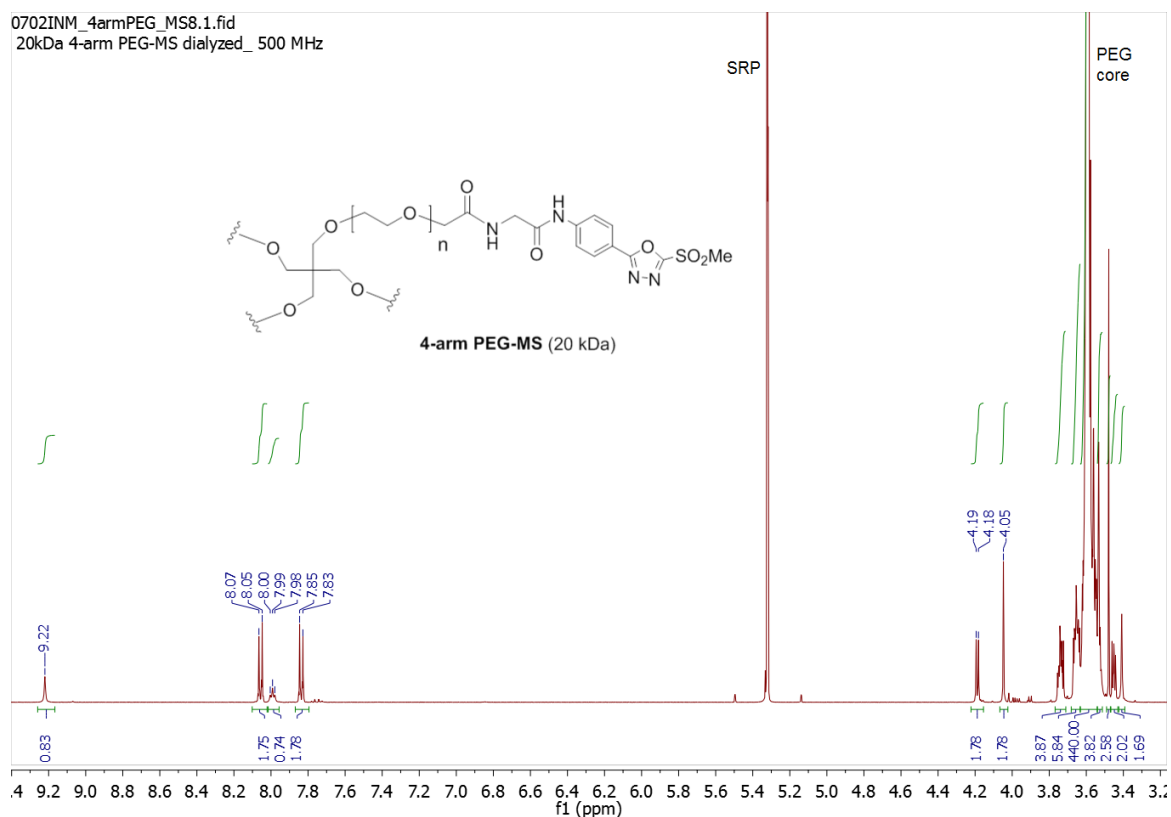


### 1.2.3. Synthesis of 4-arm PEG-MS:

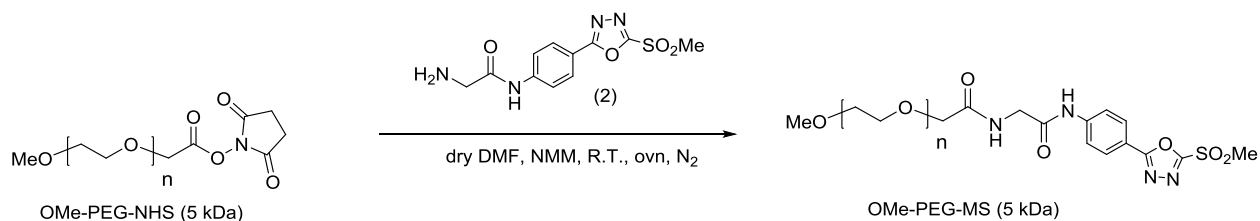


Freshly prepared compound **2** (170  $\mu$ mol, 53 mg) and N-methylmorpholine (260  $\mu$ mol, 70  $\mu$ L) were dissolved in dry DMF (3 mL), purged with nitrogen and stirred for 15 min. 20kDa, 4-arm PEG-NHS (350 mg, 17.5  $\mu$ mol) was dissolved in dry DMF (2 mL) and added to above solution under nitrogen stream. The mixture was stirred overnight at room temperature under inert atmosphere, then dialyzed in acetone and water, and freeze-dried. A white solid polymer was obtained and characterized by <sup>1</sup>H NMR in DCM-d<sub>2</sub>. Functionalization degree was calculated as 90% and yield was 85%.

<sup>1</sup>H-NMR (500 MHz, DCM-d<sub>2</sub>,  $\delta$  [ppm]) = 9.22 (s, -NH), 8.06 (pseudo-d, -CH Ar); 7.99 (pseudo-t, -NH), 7.84 (pseudo-d, -CH Ar); 4.18 (d, -CH<sub>2</sub>); 4.05 (s, -CH<sub>2</sub>C=O PEG); 3.80-3.40 (m, PEG core and -SO<sub>2</sub>Me group).



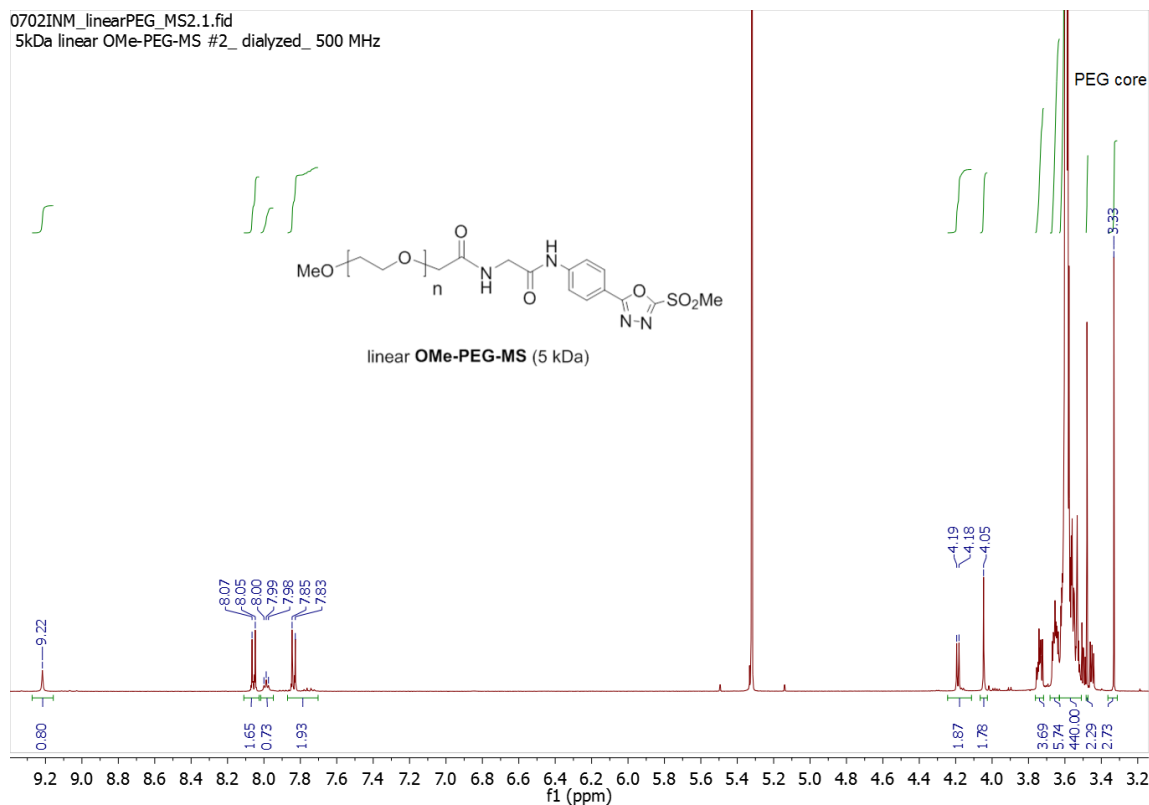
#### 1.2.4. Synthesis of linear OMe-PEG-MS:



Freshly prepared compound **2** (30 mg, 100  $\mu$ mol) was dissolved in dry DMF (3 mL) and *N*-methylmorpholine (1 mmol, 110  $\mu$ L) was added. The solution was purged with nitrogen and stirred for 15 min. 5kDa, linear OMe-PEG-NHS polymer (166 mg, 33  $\mu$ mol) was dissolved in dry DMF (2 mL) and added to the mixture under nitrogen. The mixture was reacted overnight at room temperature under inert atmosphere, dialyzed against acetone and water, and freeze-dried. A white solid polymer was obtained and characterized by <sup>1</sup>H NMR in DCM-d<sub>2</sub>. Functionalization degree was calculated as 91%, yield = 90%.

<sup>1</sup>H-NMR (500 MHz, DCM-d<sub>2</sub>,  $\delta$  [ppm]) = 9.22 (s, -NH), 8.06 (pseudo-d, -CH Ar); 7.99 (pseudo-t, -NH), 7.84 (pseudo-d, -CH Ar); 4.18 (d, -CH<sub>2</sub>); 4.05 (s, -CH<sub>2</sub>C=O PEG); 3.80-3.40 (m, PEG chain and -SO<sub>2</sub>Me group); 3.33 (-OMe PEG).

This compound was used as a linear analogue for the study in solution of thiol-MS coupling by <sup>1</sup>H NMR (Figure S1).



## 2. Additional spectroscopic characterization

### 2.1. Reaction mechanism of the thiol-MS coupling chemistry

The thiol-MS reaction is a nucleophilic aromatic substitution, where an electron-deficient aromatic ring carrying the methylsulfonyl (MS) group is the electrophile and the thiolate group is the nucleophile.<sup>[3]</sup> The MS group is expected to be expelled as the leaving group as a methanesulfinate anion (pKa 2.3).<sup>[4]</sup>

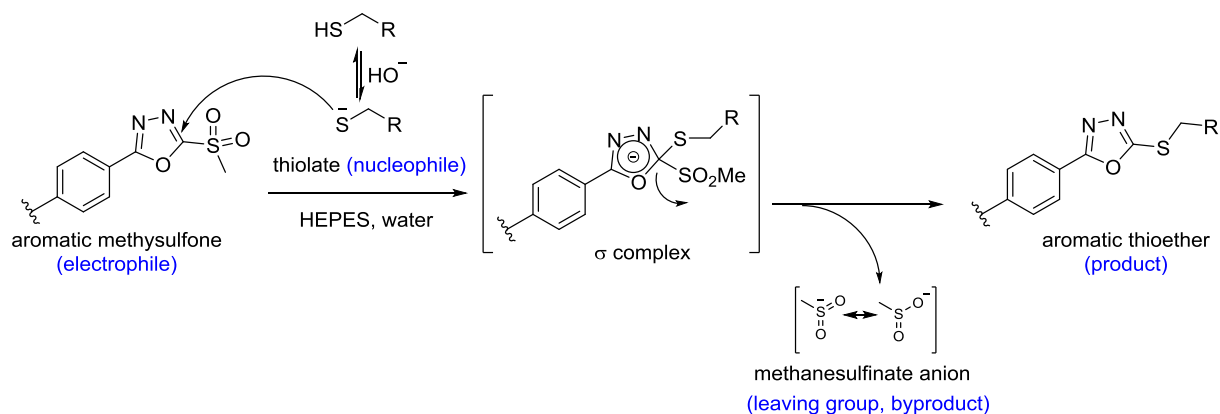


Figure S1. Mechanism of the thiol-MS reaction (nucleophilic aromatic substitution, addition-elimination).

### 2.2. Identification of the byproduct formed during thiol-MS crosslinking by <sup>1</sup>H NMR and mass spectrometry

To confirm the identity of the leaving group (expected to be the methanesulfinate anion), <sup>1</sup>H NMR and mass spectrometry analyses were performed. The coupling of 5kDa, linear PEG polymers (OMe-PEG-thiol and OMe-PEG-MS) was studied by <sup>1</sup>H NMR in deuterated d-PBS solution (pD 8, T=25°C, polymer concentration = 16mM). The PEG-thiol-MS product revealed the appearance of a new singlet signal at 2.32 ppm (Figure S2). This chemical shift matches the signal of a commercial standard solution of sodium methanesulfinate, suggesting that this new signal corresponds to the expected methanesulfinate anion as the leaving group of the reaction. To further confirm this, we analyzed by mass spectrometry (ESI-Q-TOF, negative mode) the soluble fraction produced during gel formation. A thiol-MS gel was prepared following the above procedure (40  $\mu$ L volume, 10 wt% polymer content, in 10 mM HEPES buffer, pH 8.0, T= 25°C) and the resulting gel was swollen in water (80  $\mu$ L, for about 5 min). The supernatant was collected and analyzed by mass spectrometry. We found a peak with 78.99 m/z, which matches the standard methanesulfinate anion (see Figure S3). Altogether, these results confirm that, as expected, the byproduct of the thiol-MS coupling is



the methanesulfinate anion. Importantly, no presence of methanesulfonic acid (which could be generated from methanesulfinic acid via oxidation) was detected by any of the methods.

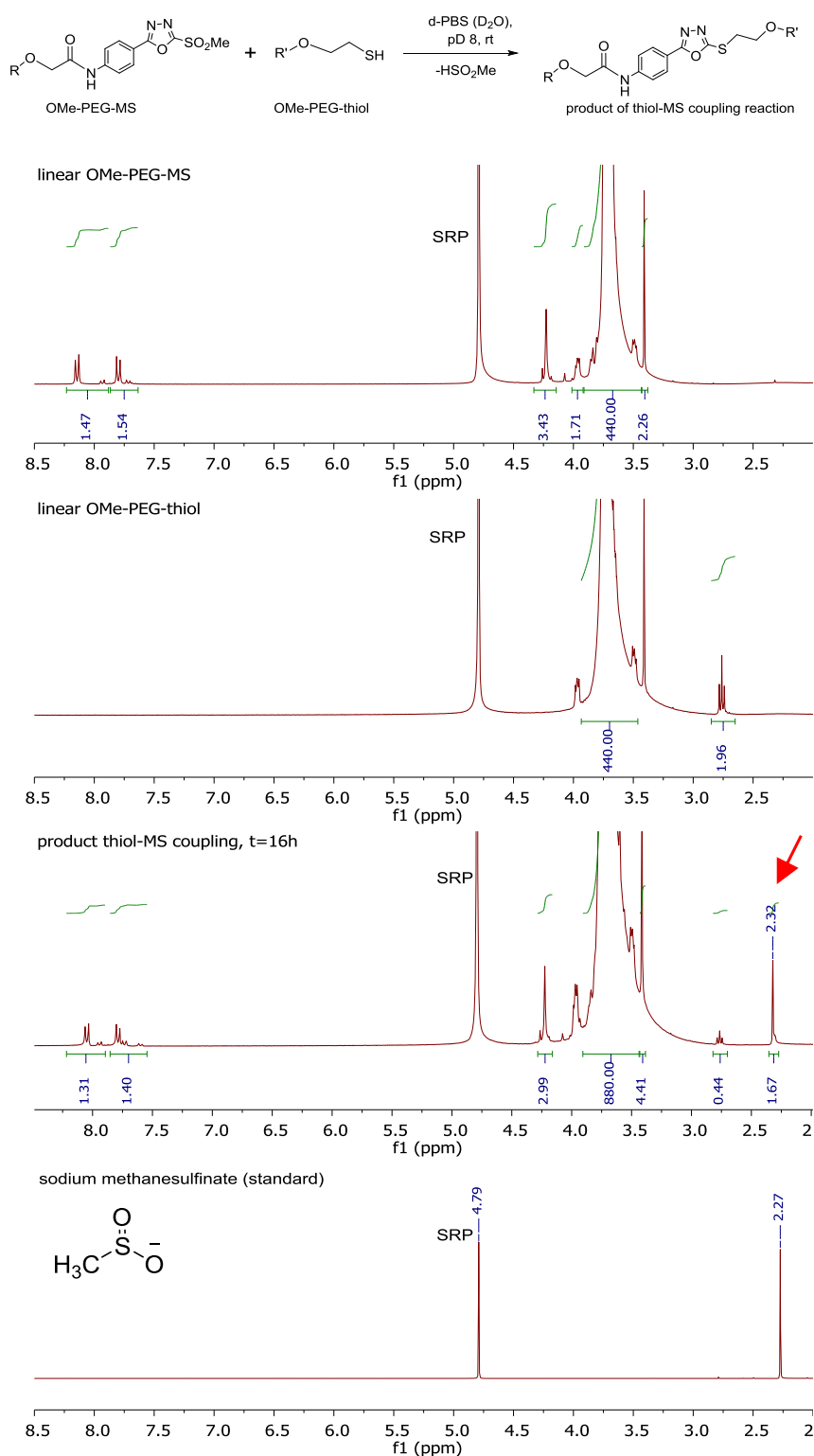


Figure S2.  $^1\text{H}$  NMR characterization of thiol-MS coupling via reaction of linear PEG polymer analogues. The red arrow indicates the new singlet signal observed during thiol-MS coupling, which chemical shift matches the standard sodium methanesulfinate. SRP means solvent residual peak.

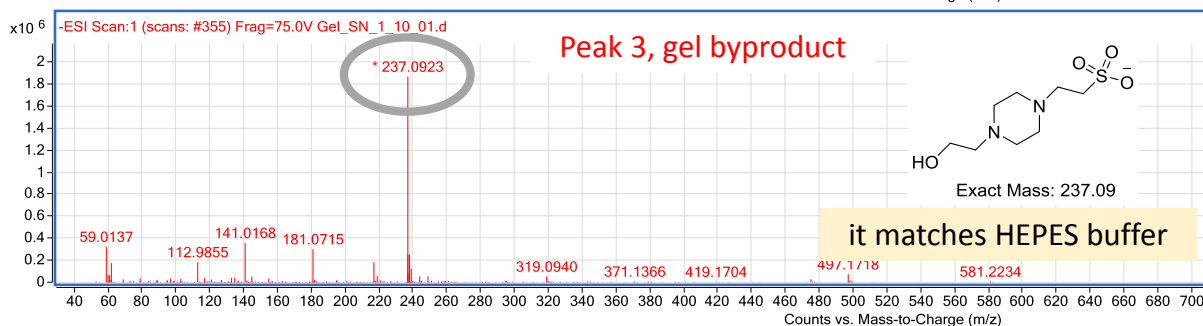
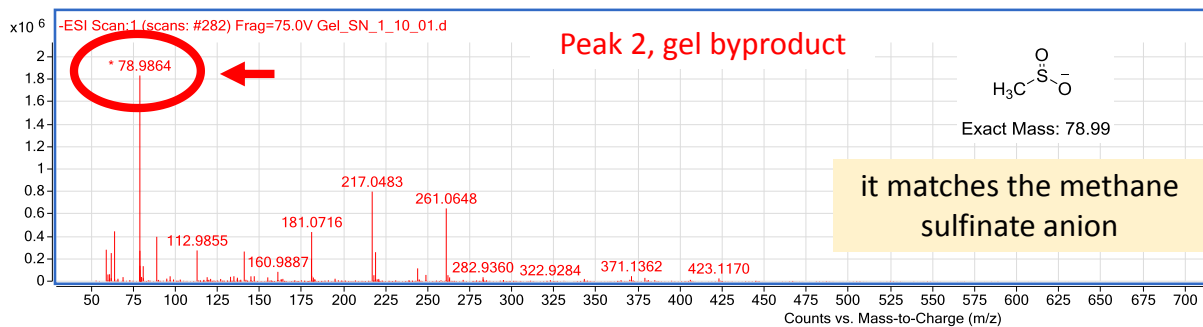
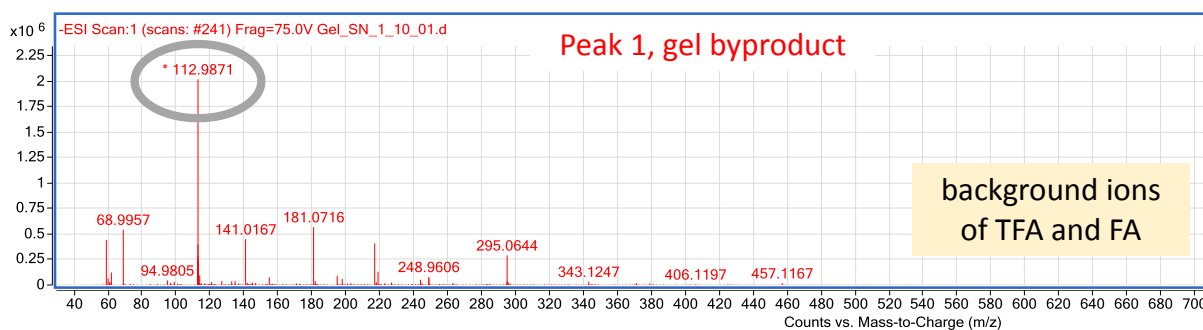
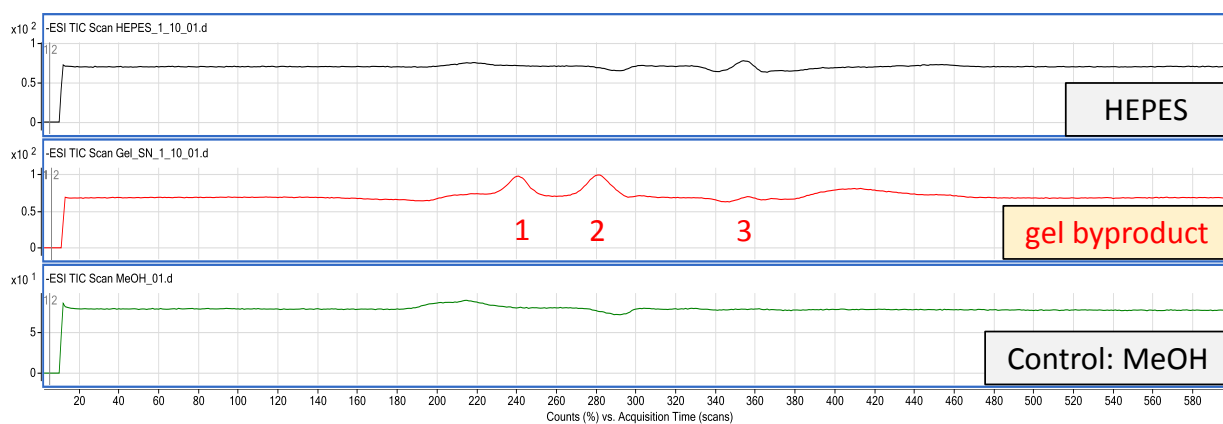


Figure S3. Mass spectrometry analysis (Q-TOF, negative mode) of the thiol-MS gel byproduct, obtained in the supernatant after swelling the gel in water for 5 min. In such solution, 3 peaks were found in the HPLC chromatogram and analyzed by mass spectrometry. The red arrow indicates the peak at 78.99 m/z, which matches the standard methanesulfinate anion.

### 2.3. Stability of Mal groups in deuterated PBS (pD 8)

The stability of Mal functional groups was measured by  $^1\text{H}$  NMR. A 40  $\text{mgmL}^{-1}$  (8 mM) solution of the linear OMe-PEG-Mal polymer was prepared in deuterated PBS, pD 8,

immediately loaded on the spectrometer and measured over time. The evolution of the integral of the signal at 6.9 ppm (corresponding to the –CH protons of Mal ring) and the appearance of new signals in the alkene region were monitored.

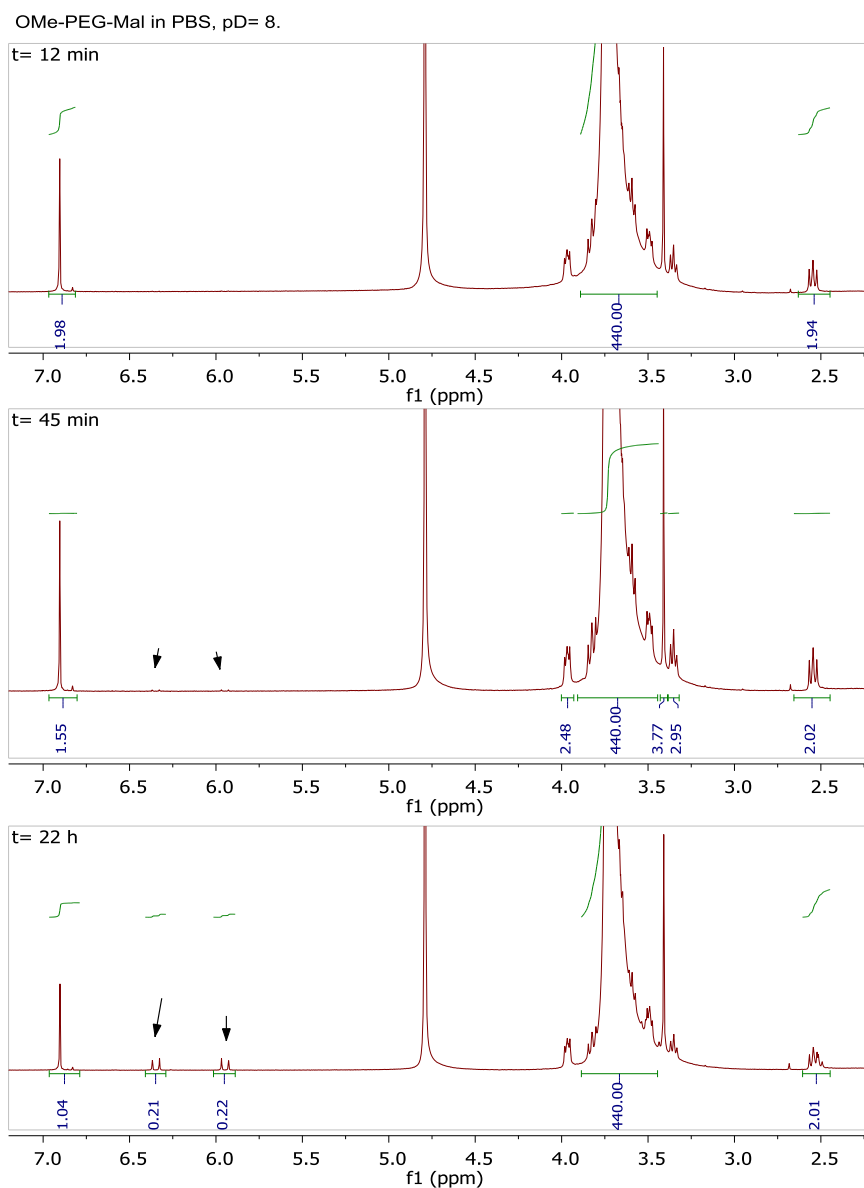


Figure S4.  $^1\text{H}$  NMR characterization of the stability of a linear OMe-PEG-Mal solution in d-PBS. The black arrows indicate the appearance of 2 new signals in the alkene region.

After 45 min, PEG-Mal showed a slight decrease in the integral of the signal at 6.9 ppm (corresponding to the –CH protons of Mal ring), and the incipient appearance of two doublets in the alkene region (6.34 and 5.95 ppm), which became more obvious after 2 h. After 22 h, the integral of the Mal signal showed a 50% decrease, and the alkene signals were noticeable. The hydrolysis of Mal group is known to occur through nucleophilic attack of the hydroxide ion to one carbonyl of the Mal ring, followed by ring opening due to C-N break.<sup>[5]</sup>

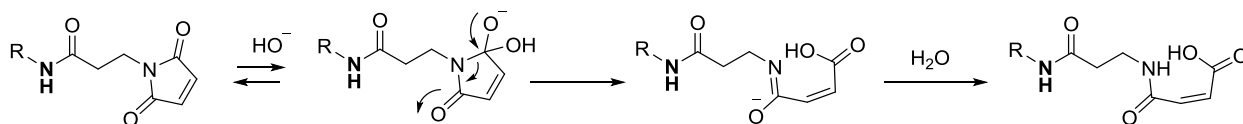


Figure S5. Mechanism of the hydrolysis of Mal groups under basic aqueous conditions. <sup>[5]</sup>

### 3. Materials characterization

#### 3.1. Rheology measurements of PEG thiol-X hydrogels

##### 3.1.1. Materials and methods

Rheological properties of hydrogels were measured on a Discovery HR-3 rheometer (TA Instruments, USA) equipped with 12 mm parallel plates and Peltier stage temperature system, typically at 25°C. For analysis, Trios v4 software was used. Data was plotted and analyzed in Origin 9.1.

20 kDa, 4-arm PEG-X polymer solutions were freshly prepared and used for these studies. The polymer was dissolved in the corresponding buffer, vortex-mixed, ultrasonicated (ca 5 s), and centrifuged to eliminate bubbles. 21  $\mu$ L of a 5 wt% PEG-X solution was loaded on the rheometer's Peltier lower plate, followed by addition of 21  $\mu$ L of a 5 wt% PEG-thiol solution and mixing with pipette tip directly on the plate. The upper plate was approached to reach a properly filled gap size of 300  $\mu$ m and the sample was sealed with paraffin or silicon oil to avoid evaporation during measurement. Total time required for sample loading and start of measurement was approximately 30-45 s.

The gelation time and final shear moduli of the hydrogel were determined. Strain sweeps (0.1 to 1000% strain at frequency = 1 Hz) and frequency sweeps (0.01 to 100 Hz at strain = 1%) were performed to determine the linear viscoelastic regime. Time sweep measurements were carried out within the linear viscoelastic regime using the following parameters: starting gap of 300  $\mu$ m, controlled axial force (0.0 $\pm$ 0.1 N), frequency 1Hz, strain 1%, temperature = 25°C.

##### 3.1.2. Statistical analysis

Data were expressed as mean  $\pm$  standard deviation (SD). For each condition, a minimum of 3 independent experiments was performed. The value of  $p < 0.05$  was used for statistical significance. A one-way analysis of variance (ANOVA) with a Tukey test of the variance was used to determine the statistical significance between groups. The statistics was performed to compare different groups and significance difference was set to  $*\alpha < 0.05$ .

### 3.2. Crosslinking of thiol-X hydrogels. Preliminary macroscopic experiments to estimate gelation time “in bulk”

20 kDa, 4-arm PEG-X polymer solutions were freshly prepared and used for these studies. The polymer was dissolved in the corresponding buffer, vortex-mixed, ultrasonicated (ca 5 s), and centrifuged to eliminate bubbles. 30  $\mu\text{L}$  of a 5% w/v PEG-X solution was placed in a plastic Eppendorf vial, followed by addition of 30  $\mu\text{L}$  of a 5% w/v PEG-thiol solution and continuous mixing with pipette (size of pipette tip= 2-200  $\mu\text{L}$ , 53 mm; from Eppendorf epT.I.P.S.®, Germany). Gelation time was taken as the time elapsed between the mixing of the two components and the moment when pipetting of the mixture was no longer possible.

### 3.3. Additional supporting results on materials characterization

#### 3.3.1. Effect of crosslinking chemistry on curing rate and mechanical properties on thiol-X hydrogels.

Hydrogels were prepared at 5 wt% polymer content, in 10 mM HEPES buffer pH 8.0 and  $T=37^\circ\text{C}$ .

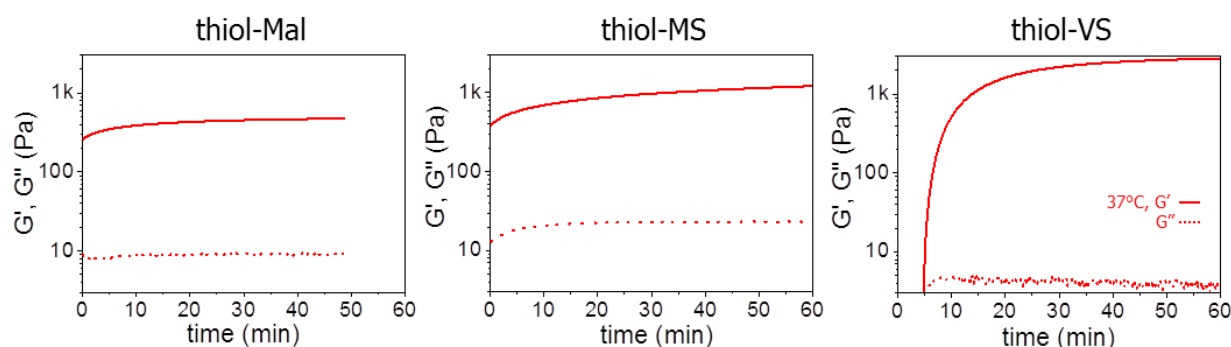


Figure S6. Rheological curves showing the curing of different thiol-X hydrogels. Conditions: 5wt% polymer, 10 mM HEPES buffer pH 8.0,  $T=37^\circ\text{C}$ .

#### 3.3.2. Effect of pH on curing rate and mechanical properties on thiol-X hydrogels

10 mM HEPES buffers at pH values of 8.0; 7.5; 7.0; and 6.6 were used for preparation of hydrogels at 5wt% polymer content and  $T=25^\circ\text{C}$ .

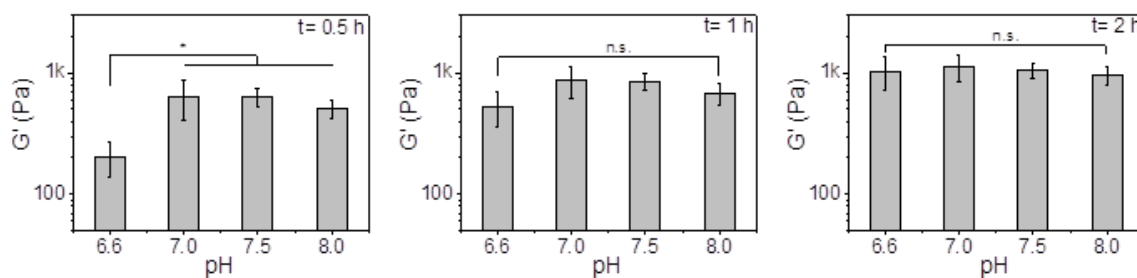


Figure S7. Effect of pH on the shear storage modulus  $G'$  of thiol-MS gels at increasing time (conditions: 5wt%, 25°C). Statistical significance analysis was performed by Tukey test (mean  $\pm$  SD, ANOVA, the value of  $*p < 0.05$  was used for statistical significance; n.s. = not significant.)

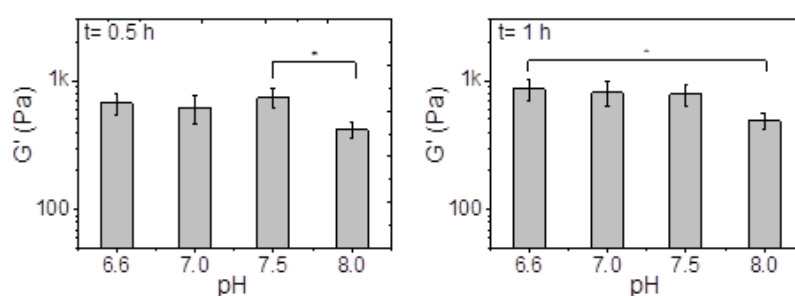


Figure S8. Effect of pH on the shear storage modulus  $G'$  of thiol-Mal gels at increasing time (conditions: 5wt%, 25°C).

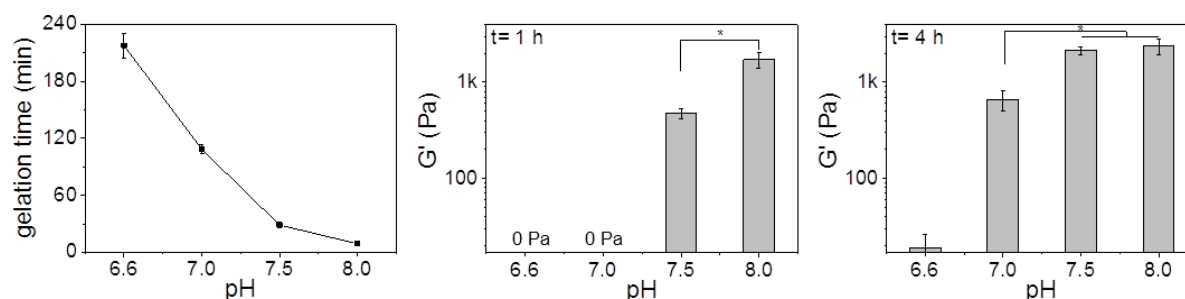


Figure S9. Effect of pH on the gelation time and shear storage modulus  $G'$  of thiol-VS gels at increasing time (conditions: 5wt%, 25°C).

### 3.3.3. Effect of temperature on curing rate and mechanical properties on thiol-MS hydrogels

Hydrogels were prepared at 5wt% polymer content, in 10 mM HEPES buffer, pH 7.0; at increasing temperatures  $T = 5-45^\circ\text{C}$ .

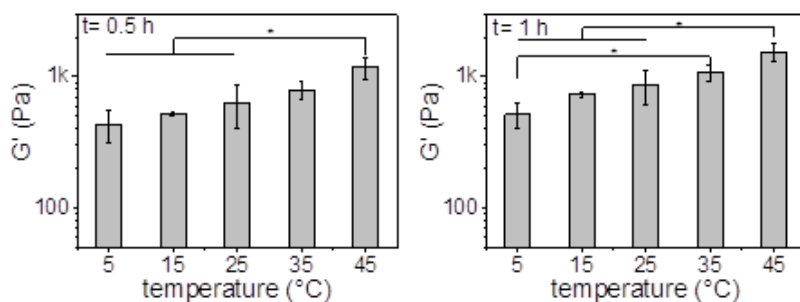


Figure S10. Effect of temperature on the shear storage modulus  $G'$  of thiol-MS gels (conditions: 5wt%, pH 7.0).

Table S1. Gelation time determined in bulk for thiol-X hydrogels at varying temperature.

gel <sup>[a]</sup>	T°			
	45°C	35°C	25°C	5°C
thiol-Mal	4 s	5 s	5-6 s	8 s
thiol-MS	7 s	10-11 s	12 s	30 s
thiol-VS	27 min	42 min	113 min	5.5 h

<sup>[a]</sup> Conditions: 5wt% polymer in 10 mM HEPES buffer pH 7.0.

### 3.3.4. Effect of polymer content and HEPES buffer concentration on thiol-MS hydrogels

Hydrogels were prepared at increasing polymer content values of 1.3; 2.5; 5.0; 7.5; and 10.0wt%; at constant pH= 7.5 and T= 25°C, at either 10 mM or 50 mM HEPES buffer concentration. The pH of resulting hydrogels was measured with a pH-meter with a flat surface electrode (PH100 Waterproof ExStik®, Extech Instruments, USA).

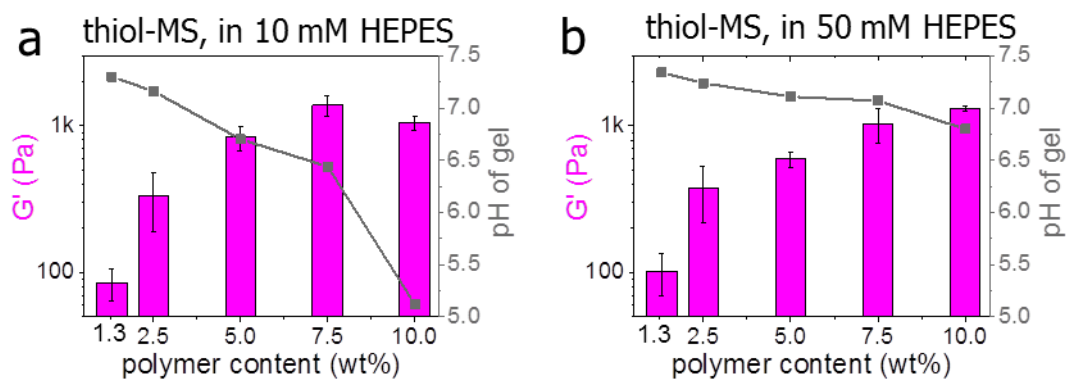


Figure S11. Effect of polymer content and HEPES buffer concentration on resulting shear storage modulus  $G'$  and pH of prepared thiol-MS gels. Conditions: 10 mM (a) and 50 mM (b) HEPES buffer, pH= 7.5, T= 25°C, at 1 h.

Table S2. Gelation time determined in bulk for thiol-X hydrogels at varying polymer content.

gel <sup>[a]</sup>	polymer content				
	10.0%	7.5%	5.0%	2.5%	1.3%
thiol-Mal	< 1 s	1-2 s	1-2 s	3 s	6 s
thiol-MS	2-3 s	4 s	6 s	10 s	18 s
thiol-VS	13 min	17 min	22 min	87 min	> 3h

<sup>[a]</sup> Conditions: in 10 mM HEPES buffer pH 7.5, T= 25°C.

### 3.4. Swelling measurements on thiol-X hydrogels

#### 3.4.1. Swelling ratio of thiol-X hydrogels

Precursor solutions of 5 wt% were prepared in 10 mM HEPES buffer pH 7.0, and chilled in ice bath. 50  $\mu$ L of a 5% w/v PEG-X solution was placed in a flexible PDMS cylindrical mold (0.75 cm diameter), quickly mixed with 50  $\mu$ L of a 5% w/v PEG-thiol solution, and allowed to crosslink in a humid chamber at 37°C for 4 h, followed by curing at room temperature overnight. The resulting hydrogels were carefully demolded and swelled in Milli-Q water at room temperature for 24 h and the mass of swollen gel was measured ( $M_s$ ). The gel was dried in oven at 40°C until constant weight (48 h) and the mass of dry hydrogel determined ( $M_d$ ). Swelling ratio (SR) was calculated according to equation S1:

$$SR = \frac{M_s - M_d}{M_d} \quad (\text{equation S1})$$

Experiments were performed in triplicate. Mean and standard deviation values were presented.

#### 3.4.2. Hydrolytic stability of thiol-X hydrogels

Following above procedure, hydrogels with 5% w/v polymer content, pH 7.0, with a total volume of 100  $\mu$ L were prepared. The resulting hydrogels were first equilibrated in Milli-Q water (24 h, 37°C) and then in medium (RPMI cell culture medium + 10%FBS + 1% P/S) (24h, 37°C). Initial mass of the swollen hydrogel was measured ( $M_i$ ). Then, the hydrogel was placed in a 24-well plate and incubated in cell culture medium (3 mL) at 37°C for 5 weeks. At



selected time points, the gel was removed from the medium, the liquid excess was blotted from the hydrogel surface carefully using a KimWipe®, and sample mass was measured ( $M_t$ ). Medium was exchanged by fresh one after each measurement. Normalized mass of swollen gel upon incubation in medium was followed over time until the physical disintegration of the sample prevented handling, and calculated according to equation S2:

$$\text{normalized mass of swollen gel} = \frac{M_t}{M_i} \quad (\text{equation S2})$$

Experiments were performed in triplicate. Mean and standard deviation values were plotted.

## 4. Cell studies

### 4.1. Cell culture conditions

Fibroblast L929 cell line (ATCC) line was cultivated at 37 °C and 5% CO<sub>2</sub> in RPMI 1640 medium (Gibco, 61870-010) supplemented with 10% FBS (Gibco, 10270) and 1% P/S (Invitrogen). For suspended cell culture, L929 cells ( $10 \times 10^6$  cells mL<sup>-1</sup>) were directly suspended in PEG precursor solution during polymerization.

For spheroid culture, a fibrin clot of Fibroblast L929 cell line was prepared by following literature reports.<sup>[6]</sup> Briefly, one pellet of  $10 \times 10^6$  cells mL<sup>-1</sup> was dissociated in fibrinogen (10 mg mL<sup>-1</sup> in PBS) and 2  $\mu$ L drops were placed on a hydrophobic Sigmacote-coated glass slide. 1  $\mu$ L thrombin solution (5 UN mL<sup>-1</sup> in PBS) was mixed with each drop of fibrinogen and the cells were placed in an incubator for 15 min to get a fibrin clot.

### 4.2. PEG Hydrogel Preparation for 3D cell culture

PEG hydrogels were prepared by adapting previously reported protocols.<sup>[7]</sup> Precursor solutions of 20kDa 4-Arm PEG Mal/VS/MS (100 mg mL<sup>-1</sup>, 10 % w/v) were prepared by dissolving in HEPES buffer (10 mM, pH 8.0) inside sterile laminar flow. Solutions of cyclo(RGDfC) (3.45 mg mL<sup>-1</sup>, 5 mM), and VPM peptide (GCRDVPMSMRGGDRCG, 26.6 mg mL<sup>-1</sup>, 15.68 mM) were also prepared in sterile HEPES buffer (pH 8.0). These concentrations were kept constant during all cell experiments.

4-Arm-PEG Mal/MS/VS stock solution (10 % w/v) was mixed in 2:1 volume ratio with 5 mM cyclo(RGDfC) and incubated for 30 min at 37 °C. The cell suspension ( $10 \times 10^6$  cells mL<sup>-1</sup>) in RPMI medium (2  $\mu$ L) was added to the above solution and 8  $\mu$ L drops of resulting mixture were placed in an Ibidi 15- $\mu$ well angiogenesis slide. Immediately, the solution of VPM

peptide (2  $\mu\text{L}$ , 15.8 mM) was added to each  $\mu\text{-well}$ , carefully mixed with pipette tip and allowed to crosslink. Mal and MS hydrogels were let to polymerize for 15 min, while VS hydrogels were let to polymerize for 45 min at 37 °C and 5%  $\text{CO}_2$ . After gelation, RPMI medium was added and culture was maintained for 1-3 days. Alternatively, for spheroid culture, RPMI medium (2 $\mu\text{L}$ ) was mixed with cyclo(RGDfC) modified PEG-precursor solution (6  $\mu\text{L}$ , as described above) and added (8 $\mu\text{L}$ ) to each to  $\mu\text{-well}$ . One fibrin clot was added to each well, followed by the addition of 15.8 mM VPM peptide (2  $\mu\text{L}$ ) and allowed to gelate for 15-45 mins at 37 °C. Medium (50  $\mu\text{L}$ ) was added to each well and substituted by fresh medium every 24 h during cell culture.

#### **4.3. Live/dead Assay**

Cell culture medium was removed, and samples were incubated for 5 min with fluorescein diacetate (40  $\mu\text{g mL}^{-1}$ ) and propidium iodide (30  $\mu\text{g mL}^{-1}$ ) in PBS. Samples were washed twice with PBS and imaged with Zeiss LSM 880 confocal microscope.

#### **4.4. Fixation and Staining**

3D PEG hydrogel samples were fixed with 4% PFA solution for 2 h at room temperature and washed with PBS. Samples were blocked with 1% BSA solution for 1 h, followed by permeabilization with 0.5% Triton X-100 for 1 h. FITC-phalloidin (1:200 in water, Thermo Fisher Scientific) was used for staining actin fibers and DAPI (1:500 in water, Life Technology) for staining nucleus. Samples were incubated with antibodies for 5 h at room temperature followed by washing with PBS.

#### **4.5. Migration assay**

Cell migration assay indicates ease of cell motility in a 3D matrix and is a measurement of distance travelled by leading cells from encapsulated spheroids. Migration distance of cell from spheroid was analyzed from confocal z-stack of spheroids taken after fixation and staining. The distance from the apical tip of a leading cell to the center of spheroid was measured in all directions in each slice (5 $\mu\text{m}$ ) of z-stack (~150-200 cells/samples) by using Zen-blue software to calculate average distance covered by cells in the different PEG Mal/VS/MS hydrogels.

#### **4.6. Statistical Analysis**

All experiments comprised of at least three independent experimental batches. Data are expressed as means  $\pm$  SD. Cell viability was calculated from fluorescence images taken after treatment with fluorescein diacetate and propidium iodide. For each sample, at least 5 independent z-stacks at 20x magnification were analyzed (~1200-1400 cells per sample). Live and dead cells were counted manually in each slice (3  $\mu$ m) of z-stack to calculate percentage viability of each sample.

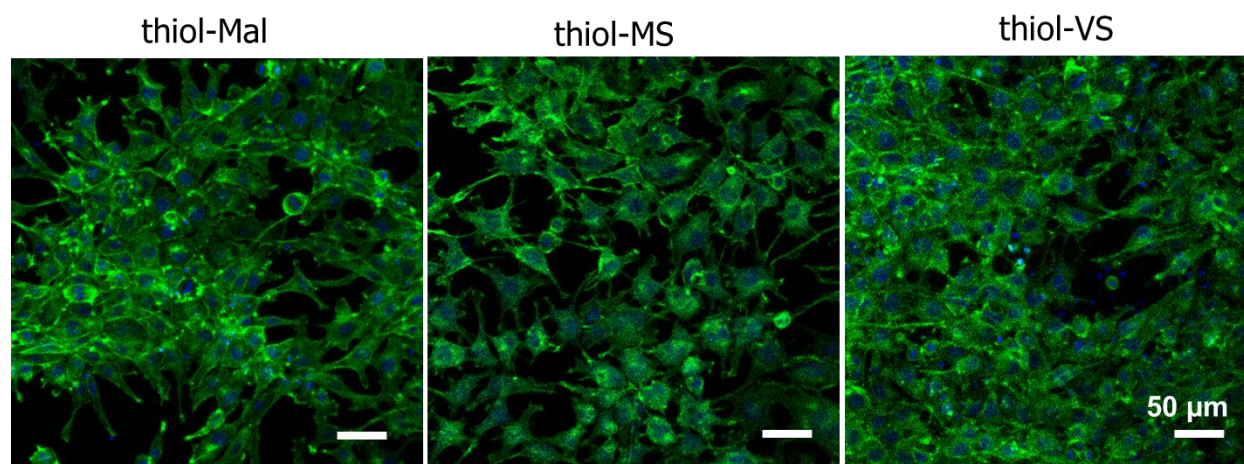


Figure S12. Morphology of single cells (mouse fibroblast L929) encapsulated into the different enzymatically cleavable thiol-X hydrogels, after 3 days of culture. In comparison to the other systems, cells cultured in thiol-MS hydrogels showed more homogeneous distribution, less clustering or aggregation. Color code: green: FITC-phalloidin (actin fibers), blue: DAPI (nucleus).

#### 4.7. Cytocompatibility of 50 mM HEPES buffer solution

L929 fibroblasts were cultured (overnight, 37°C, in a humidified atmosphere containing 5% CO<sub>2</sub>) on cell culture plate, in medium containing 50 mM HEPES buffer and RPMI 1640 medium (Gibco, 61870-010) supplemented with 10 % Fetal Bovine Serum (Gibco, 10270) and 1% antibiotics (penicillin/streptomycin) (Invitrogen); final pH= 7.5. Live/dead assay was performed.

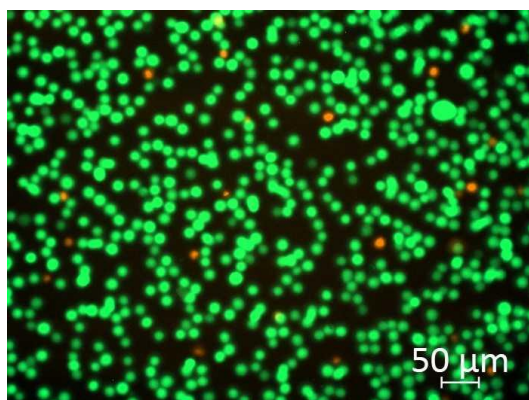


Figure S13. Live (green)/ dead (red) assay of L929 fibroblasts cultured overnight in cell culture medium containing 50 mM HEPES buffer, pH 7.5.

### References of Supporting Information

- [1] A. K. Covington, M. Paabo, R. A. Robinson, R. G. Bates, *Analytical Chemistry* **1968**, 40, 700.
- [2] a) Z. Zheng, G. Li, C. Wu, M. Zhang, Y. Zhao, G. Liang, *Chemical Communications* **2017**, 53, 3567; b) X. Zhao, G. Lv, Y. Peng, Q. Liu, X. Li, S. Wang, K. Li, L. Qiu, J. Lin, *ChemBioChem* **2018**, 19, 1060.
- [3] a) D. Zhang, N. O. Devarie-Baez, Q. Li, J. R. Lancaster, M. Xian, *Organic Letters* **2012**, 14, 3396; b) N. Toda, S. Asano, C. F. Barbas, *Angew. Chem., Int. Ed.* **2013**, 52, 12592.
- [4] F. Wudl, D. A. Lightner, D. J. Cram, *Journal of the American Chemical Society* **1967**, 89, 4099.
- [5] R. G. Barradas, S. Fletcher, J. D. Porter, *Canadian Journal of Chemistry* **1976**, 54, 1400.
- [6] a) S.-H. Lee, J. J. Moon, J. L. West, *Biomaterials* **2008**, 29, 2962; b) C. A. DeForest, K. S. Anseth, *Nature chemistry* **2011**, 3, 925.
- [7] a) E. A. Phelps, N. O. Enemchukwu, V. F. Fiore, J. C. Sy, N. Murthy, T. A. Sulchek, T. H. Barker, A. J. García, *Advanced Materials* **2012**, 24, 64; b) A. Farrukh, J. I. Paez, A. del Campo, *Advanced Functional Materials* **2019**, 29, 1807734.

SupplInformation\_PaezJI.pdf (1.84 MiB)

[view on ChemRxiv](#) • [download file](#)

---